Caisson structures in the Beaufort Sea 1982-1990 : Characteristics, instrumentation and ice loads

Timco, G. W.; Johnston, M. E.

Publisher's version / Version de l'éditeur:
https://doi.org/10.4224/12328162
Technical Report, 2002-11

Caisson Structures in the Beaufort Sea 1982-1990:
Characteristics, Instrumentation and Ice Loads

G.W. Timco and M.E. Johnston
Canadian Hydraulics Centre
National Research Council of Canada
Ottawa, Ont. K1A 0R6
Canada

Technical Report
CHC-TR-003

November 2002

ABSTRACT

This report presents a comprehensive overview of the characteristics, instrumentation and measured ice loads on the caisson structures that were used for exploratory drilling in the Canadian Beaufort Sea in the 1970s and 1980s. Details are presented on the Tarsiut Caissons, the Single Steel Drilling Caisson (SSDC), the Caisson Retained Island (CRI), and the Molikpaq. Details on the ice-load measuring instrumentation are presented for each of the drill sites where an ice-load measurement program took place. The global loads on the structures are presented as a Line Load (Global Load per width of the structure) and the Global Pressure (Line Load per ice thickness). Global loads are shown to be a function of the ice macrostructure (level first-year sea ice, multi-year ice, first-year ridges, hummock fields, isolated floes). The analysis shows that there is a general increase in the Line Load with increasing ice thickness. The data show considerable scatter. Much of the scatter can be explained by examining the failure mode of the ice during the interaction process. The most significant result of the analysis shows that the maximum Global Pressure measured for all types of ice loading events never exceeded 2 MN/m^2.

TABLE OF CONTENTS

LIST OF FIGURES

LIST OF TABLES

Caisson Structures in the Beaufort Sea 1982-1990:
Characteristics, Instrumentation and Ice Loads

1.0 INTRODUCTION

During the 1970s and 1980s there was considerable activity for oil exploration in the Canadian and American Beaufort Sea. Over 140 wells were drilled using innovative technology that evolved with time. This evolution was a result of a better understanding of the Arctic environment and the need to operate in increasingly deeper waters with more extreme ice conditions. Initially during this exploration, the knowledge of actual ice loads on wide structures was virtually non-existent. Because of this, many of the structures were instrumented to measure the ice loads, and active and invaluable measurement programs were developed.

When the Beaufort Sea activity declined in the early 1990s, the Oil Industry redirected its interests to other regions. Since there was a fear that the information and knowledge of the ice loads might be lost, the National Research Council in Ottawa approached the Oil Industry to gain access to, archive, and use this information. The Industry was very responsive to this request and the NRC set-up a Centre of Ice Loads on Structures (Timco 1996, 1998). The Program on Energy Research and Development (PERD) provided funding for this project. The NRC obtained reports, data, and videos from Gulf Canada Resources Ltd., Imperial Esso, and Dome Petroleum (Canmar). At the present time, there are over 2000 reports, 300 films and videos, and original data from the Molikpaq and the Single Steel Drilling Caisson (SSDC). The NRC actively uses this information to better understand ice loads on offshore structures (Frederking et al., 1999; Timco et al., 1999a, 1999b; Timco and Wright, 1999; Wright and Timco, 2000).

Recently, there has been interest in continuing exploration of the Beaufort Sea. The intent of this report is to provide an overview of the drilling activity in the 1980s and 1990s. Particular emphasis is given to the ice loads measured on the caisson-type structures.

2.0 OVERVIEW OF BEAUFORT SEA STRUCTURES

There have been several approaches used to design platforms for oil exploration in the Arctic regions. In the Beaufort Sea, off both Canada and Alaska, over 140 wells have been drilled. Innovative technology and good management have allowed exploration of this region. The exploration took place over a fairly short time span. A number of the major oil companies were involved in this venture. There was both competition and collaborative work to investigate the ice loads and types of structures that could be used. This section details the structures that were used.

2.1 Artificial Islands

The development of the Beaufort was initiated in the early 1970s in quite shallow water (up to 12 m) using artificial islands. These islands were constructed by either dredging the local sea bottom and building-up an island, or by trucking gravel from the shore and dumping it to form an island. For most of these islands, the ice was landfast, first-year ice and had little movement during the winter months. In the early 1970s, Esso Resources Canada Ltd. and Exxon Production Research measured the *in-situ* ice pressures around their dredged exploration drilling islands at Adgo, Netserk, Arnak, Kannerk and Issungnak (see Figure 1 and Figure 2). Urethane button-type sensors were used to measure the pressure, with supplementary information on ice/island movements. These measurement programs often experienced electrical and environmental difficulties and little data are available from them in the open literature. The successful measurements indicated, however, that the ice load was applied relatively uniformly across the Island, with loading times on the order of one day. The field studies indicated that pressures up to about 1 MPa were measured on this type of structure (Ralston, 1979).

2.2 Floating Drillships

Starting in the mid 1970s, Dome Petroleum (Canmar) deployed floating drillships during the summer months (Figure 3). These were moored on site during the summer (open water) months. They encountered relatively light ice conditions, and there are no recorded ice loading events for these floating structures.

In 1983, Gulf Canada Resources Ltd. designed and built an inverted-cone shaped floating structure (the “Kulluk”) that allowed drilling later into the winter season. This structure was exposed to moving pack ice. Active ice management around the Kulluk ensured that the ice conditions were not severe (see Figure 4). This structure was instrumented to measure mooring line forces. Wright (2000, 2001) summarized the measured forces on the Kulluk. Measured loads were up to 4 MN depending upon the ice thickness, floe size and ice concentration.

Figure 1: Photograph of sandbag protected artificial island

Figure 2: Photograph of the Esso artificial island at Issungnak

Figure 3: Photograph of a Canmar drillship

Figure 4: Photograph showing the ice management around the moored Kulluk structure in the Beaufort Sea.

2.3 Caisson Structures

In the early 1980s, five special-built caisson structures were designed and built to allow year-round drilling and development of regions further offshore in harsher ice conditions. There were five different caisson structures used in Arctic regions:

- Tarsiut Caisson
- Single-Steel Drilling Caisson (SSDC)
- Caisson-Retained Island (CRI)
- Molikpaq
- Glomar Beaufort Sea I (CIDS)

Table 1 provides some details on their characteristics, based on the paper by Masterson et al. (1991). The caisson structures are discussed in detail in later chapters of this report.

Table 1: Details of the Fixed Structures used in Arctic Drilling

	Tarsiut	SSDC	CRI	Molikpaq	CIDS
Drilling Days (per year)	365	365	365	365	365
Base Area (m^2) (including core)	7947	18590	10875	12383	8551
Oceanographic Limitations (wave height - m)	12	12.2	15	12.2	5.2
Limiting Level Ice Conditions (m)	5.6	10	3	10	2
Ice Concentrations	10/10s	10/10s	10/10s	10/10s	10/10s
Design Ice Load - Global (MN)	560	900	436	640	640
Design Local Ice Pressure (MPa)	4.1	8.3	2.8	3.0	6.2
Area for Local Pressure (m^2)	3.7	3.7	0.7	2.3	2.3
Wells Drilled	Tarsiut N-44 Tarsiut N-44A	Uviluk P-66 Kogyuk N-67 Phoenix #1 Aurora #1	Kadluk O-07 Amerk O-09 Kaubvik I-43	Tarsuit P-45 Amauligak I-65 Amauligak I-65A Amauligak I-65B Amauligak 2F-24 Amauligak 2F-24A Amauligak F-24 Amauligak 2F-24B Isserk I-15	Antares #1 Antares #2 Orion #1

2.4 Spray Islands

In the late 1980s, spray ice islands (Figure 5 and Figure 6 after Poplin, 1990) were used for a few wells. These were deployed in landfast ice in both the Alaskan and Canadian Beaufort Sea. The cost of these spray islands was approximately one-half the cost of a gravel island.

Figure 5: Photograph showing an overview of the Nipterk spray island.

Figure 6: Photograph showing the Nipterk spray island from ice level.

2.5 Overview of Drilling Activity

There were 88 wells drilled in the Canadian Beaufort Sea. Table 2 lists some of the salient details of these wells (from Masterson et al., 1991).

Table 2: Drilling Activity in the Canadian Beaufort Sea

Year	Well Name	Operator	Drill Vessel	Water Depth (m)	Spud Date	Rig Release
1972	Roland Bay L-41	Pacific	---	20.1	72/12/22	73/04/20
1973	Immerk B-48	Imp	Sacrificial beach	3.0	73/09/17	73/12/22
	Adgo F-28	Esso	Sandbag retained	2.0	73/12/28	74/03/19
1974	Pullen E-17	Imp	Sandbag retained	1.5	74/04/21	74/07/11
	Unark L-24	Sun/BVX	Hauled Island	1.5	74/09/26	75/05/24
	Pelly B-35	Sun/BVX	Hauled Island	1.5	74/11/05	75/02/14
1975	Adgo P-25	Esso	Sandbag retained	2.0	75/01/02	75/03/28
	Nerlerk B-44	Imp	Sandbag retained	4.6	75/01/06	75/06/08
	Adgo C-15	Esso	Sandbag retained	2.0	75/04/21	75/07/25
	Garry P-94	Sun/SOBC/BVX	Hauled Island	2.5	75/08/25	76/01/05
	Ikattok J-17	Imp/Delta	Sandbag retained	2.0	75/10/07	76/02/28
	Nerlerk F-40	Imp	Sandbag retained	7.0	75/11/08	76/05/09
1976	Sarpik B-35	Imp	Sandbag retained	3.5	76/04/02	76/09/04
	Kopanoar D-14	Hunt/Dome	Drill Ship	60.3	76/08/08	76/09/26
	Nektoralik K-59	Dome/Hunt	Drill Ship	34.0	76/09/21	77/10/17
	Kugmallit H-59	Imp	Sandbag retained	5.2	76/09/30	76/11/10
	Arnak L-30	Imp	Sacrificial beach	8.5	76/10/05	77/03/16
	Tingmiark K-91	Dome/Gulf	Drill Ship	27.3	76/10/18	77/10/25
	Unark L-24A	Sun/BVX	Hauled Island	1.5	76/10/19	77/05/08
1977	Kannerk G-42	Imp/IOE	Sacrificial beach	8.0	77/03/30	77/05/13
	Ukalerk C-50	Dome/Gulf	Drill Ship	20.0	77/07/18	77/10/03
	Kopanoar M-13	Dome	Drill Ship	59.5	77/07/19	79/xx/xx
	Nerlerk M-98	Dome	Drill Ship	52.0	77/10/07	79/08/28
	Isserk E-27	Esso	Sacrificial beach	13.0	77/12/04	78/05/05
1978	Garry G-07	Sun/CCL/BVX	Hauled Island	2.5	78/02/10	78/05/13
	Natsek E-56	Dome//Petrocan	Drill Ship	34.1	78/07/10	79/10/16
	Ukalerk 2C-50	Dome/Gulf	Drill Ship	20.0	78/08/10	79/10/11
	Tarsuit A-25	Gulf	Drill Ship	20.0	78/10/18	80/07/28
	Kaglulik M-64	Dome	Drill ship	31.0	78/11/03	79/07/10
	Kaglulik A-75	Dome	Drill ship	32.6	78/xx/xx	78/xx/xx
1979	Adgo J-27	Esso	Sandbag retained	2.0	79/04/05	79/08/07
	Kenalooak J-94	Dome	Drill ship	49.3	79/09/20	82/11/01
	Kopanoar L-34	Dome	Drill Ship	60.0	79/10/11	79/11/25
	Koakoak O-22	Dome	Drill ship	49.2	79/11/05	81/10/31
	Kopanoar 2L-34	Dome/Gulf	Drill Ship	60.3	79/11/25	79/11/28
1980	Kilannik A-77	Dome	Drill ship	23.7	80/06/23	81/09/04
	Kapanoar I -44	Dome/Gulf/Hunt	Drill Ship	58.0	80/07/10	80/08/01
	Kopanoar 2I-44	Dome/Gulf	Drill Ship	57.9	80/08/03	80/10/29
	Issungnak 2 O-61	Esso	Sacrificial beach	18.6	80/10/02	81/08/13
1981	Issugnak L-86	Gulf	Drill ship	18.6	81/07/17	81/10/16
	Alerk P-23	Esso	Sacrificial beach	11.6	81/09/21	81/12/24
	Irkaluk B-35	Dome/Hunt	Drill ship	60.3	81/09/28	82/10/04
	Tarsuit N-44	Gulf	Caisson-concrete	19.2	81/12/11	82/06/07

Table 2 (cont'd): Drilling Activity in the Canadian Beaufort Sea

Year	Well Name	Operator	Drill Vessel	Water Depth (m)	Spud Date	Rig Release
1982	Issugnak O -61	Esso	Sacrificial beach	36.5	82/02/06	80/07/08
	West Atkinson L-17	Esso	Sandbag retained	7.0	82/05/01	82/06/25
	Tarsuit N-44A	Gulf	Caisson-concrete	19.2	82/06/18	82/09/19
	Kiggavik A-43	gulf	Drill ship	27.4	82/08/20	82/10/17
	Orvilruk O-03	Dome/Superior	Drill Ship	59.9	82/08/30	82/10/25
	Aiverk I-45	Dome	Drill ship	50.3	82/10/07	82/10/23
	Aiverk 2I-45	Dome	Drill ship	50.3	82/11/03	84/10/11
	Itiyok I-27	Esso	Sacrificial beach	14.0	82/11/05	83/05/02
	Uviluk P-66	Dome/Texaco	SSDC	30.0	82/11/10	83/05/21
1983	Natiak O-44	Dome	Drill Ship	44.0	83/07/16	84/09/25
	Havik B-41	Dome	Drill ship	35.0	83/07/17	86/08/24
	Siulik I-05	Dome	Drill Ship	49.4	83/07/25	84/10/18
	Arluk E-90	Dome	Drill ship	58.0	83/07/30	85/10/13
	Pitsiulak A-05	Gulf	Kulluk	27.0	83/08/22	84/07/26
	Kadluk O-07	Esso	CRI	13.6	83/09/25	84/04/24
	Kogyuk N-67	Gulf	SSDC	28.4	83/10/28	84/01/30
	Amauligak J-44	Gulf	Kulluk	19.5	83/11/16	84/09/23
1984	Amerk O-09	Esso	CRI	26.0	84/08/22	85/03/03
	Nerlerk J-67	Dome	Kulluk	45.0	84/09/16	85/10/24
	Tarsuit P-45	Gulf	Milikapq	22.4	84/09/25	84/12/24
	Adgo H-29	Esso	Sandbag retained	3.0	84/09/27	85/01/12
	Nipterk L-19	Esso	Sacrificial Beach	11.3	84/10/03	85/03/23
	Akpak P-35	Gulf	Kulluk	20.0	84/10/17	84/11/08
1985	Nipterk L-19A	Esso	Sacrificial Beach	11.3	85/04/21	85/07/15
	Akpak 2P-35	Gulf	Kulluk	20.0	85/06/10	85/07/07
	Adlartok P-09	Dome	Drill ship	67.4	85/08/08	85/10/17
	Edlok K-56 N-56	Dome	Drill ship	31.5	85/08/10	85/09/16
	Amauligak I-65	Gulf	Molikpaq	22.9	85/09/24	86/01/28
	Adgo G-24	Esso	Sandbag retained	1.4	85/10/07	86/01/07
	Aagnerk E-56	Gulf	Kulluk	20.0	85/10/28	86/06/26
	Minuk I-53	Esso	Sacrificial Beach	14.7	85/11/27	86/05/02
	Ellice L-39	Chev/Tril	Sandbag retained	2.0	85/xx/xx	86/04/20
1986	Amauligak I-65A	Gulf	Molikpaq	22.8	86/01/28	86/03/20
	Amauligak I-65B	Gulf	Molikpaq	22.9	86/03/20	86/09/19
	Arnak K-06	Esso	Sacrificial beach	7.6	86/04/27	86/08/12
	Kaubvik I-43	Esso/Home	CRI	17.9	86/10/22	87/01/10
1987	Angasak L-03	Tril/Esso/Chevron	Spray ice island	5.4	87/02/24	87/04/12
	Amauligak 2F-24	Gulf	Molikpaq	26.5	87/12/22	88/01/29
1988	Amauligak 2F-24A	Gulf	Molikpaq	26.6	88/01/30	88/02/17
	Amauligak F-24	Gulf	Molikpaq	26.6	88/04/13	88/08/12
	Amauligak 2F-24B	Gulf	Molikpaq	26.6	88/04/15	88/08/07
	Amauligak O-86	Gulf	Kulluk	20.0	88/06/30	88/08/26
1989	Nipterk P-32	Esso/Chevron	Spray Ice Island	6.7	89/02/21	89/04/20
	Isserk I-15	Esso/Gulf	Molikpaq	11.5	89/11/11	90/01/08
	Kingark J-54	Amoco	Drill ship	30.0	89/xx/xx	90/xx/xx

Figure 7 has been produced from the information in this table. It shows a "flow chart" overview of the drilling activity in the Canadian Beaufort Sea. Note the progression from seasonal artificial islands and drill ships to the more robust caisson-type structures.

Figure 7: Overview of drilling activity in the Canadian Beaufort Sea.

Significant oil and gas discoveries were made in the Beaufort Sea (see Figure 8), including the Amauligak oil reservoir. To date, these reserves have not been developed. Current discovered reserves for this region are 12 TCF gas, and 1.6 billion Bbls of oil. During the drilling of the Amauligak well, 320,000 barrels of oil were shipped to Japan in the tanker "Gulf Beaufort", making it the first major shipment of crude oil from the Canadian Beaufort Sea.

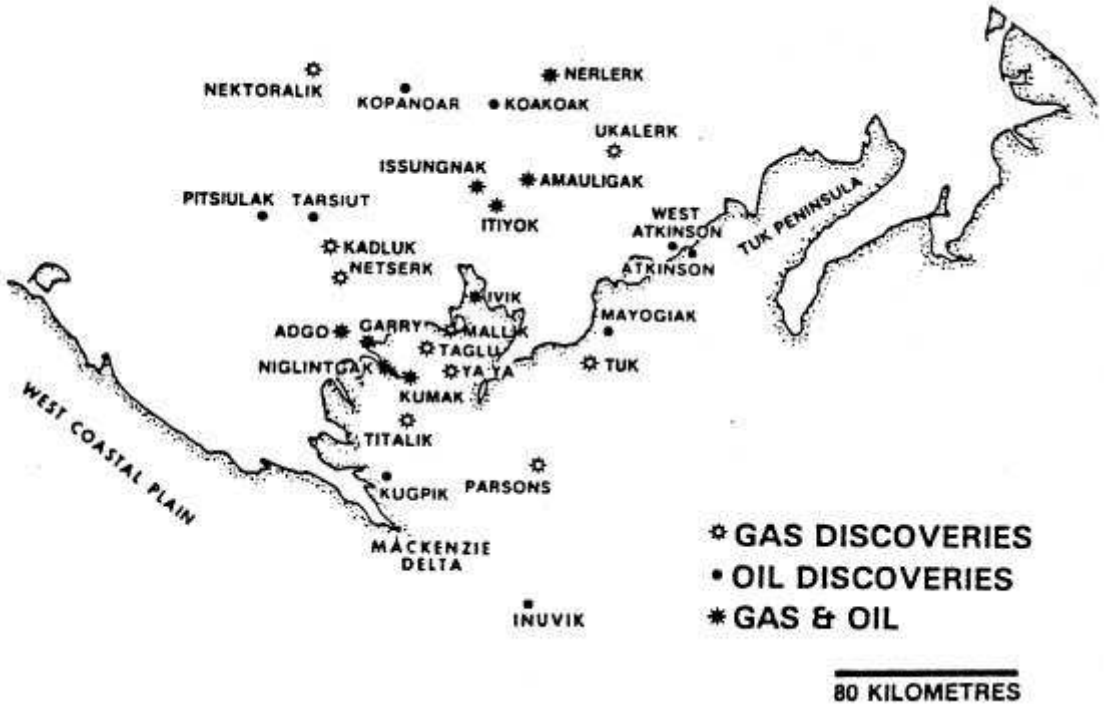

Figure 8: Map showing the gas and oil discoveries in the Canadian Beaufort Sea (after Jahns 1985).

2.6 Definition of Terms

As previously mentioned, the intent of this report is to provide an overview of the drilling activity in the 1980s and 1990s with particular emphasis on the ice loads on caisson-type structures. Before doing this, it is important to understand the format of the data presentation and define the approach that will be used.

The caisson structures were all quite wide (typically 100 m width). The measurement of loads was done by placing several sensors along the face of the structure. Then, by knowing the area covered and using extrapolation techniques, the loads were determined. For presentation here, these global loads were normalized by the width of the structure loaded by the ice. This is defined as a “Line Load” where

$$Line\ Load = \frac{Measured\ Global\ Load}{Width\ of\ \ Structure\ loaded\ by\ the\ Ice}$$

Using this approach provides a coherent method to compare the data. Note that the measured global load was in most cases normalized by the full width of the structure at the waterline. In a few cases, the loads were measured over only one face of the caisson, and so the face width was used as the normalizing width.

In addition, the load information is presented by introducing the concept of a "Global Pressure". This is defined as:

$$Global\ Pressure = \frac{Measured\ Global\ Load}{Width\ of\ \ Structure\ loaded\ by\ the\ Ice\ x\ Ice\ Thickness}$$

Thus, this is the Line Load normalized by the ice thickness. It should be emphasized that the values of Global Pressure should only be used in the context of the global loads on a structure. Local pressures would be considerably higher than the Global Pressure values reported here. This approach is used as a simple means to compile and compare the global load results for different structures and ice types.

3.0 TARSIUT CAISSONS

Gulf Canada Resources Ltd. operated this structure and it was the first caisson-type structure used in the Arctic. It drilled the Tarsiut N-44 well in 1981-82 (see Figure 8). During the winter of 1982-83, it was left on-site and used as a test platform to study ice interaction with a wide offshore structure. This project was known as the Tarsiut Island Research Program (TIRP).

3.1 Description of the Tarsiut Structure

The structure consists of four individual concrete caissons. These caissons were floated to the drilling site and ballasted down with sand to form a square. The inner core was filled with dredge material (see Figure 9). This structure is not regarded as a "mobile" structure since the difficulty of resetting and connecting four caissons limits its mobility. The structure is about 100 m across at the water line and has a vertical outer surface (Figure 10). The caissons are 10 m high and rest on a berm that comes to within 6 m of the water surface. The structure was extensively instrumented to measure ice loads (Pilkington et al., 1983) both for operational safety reasons and for future design.

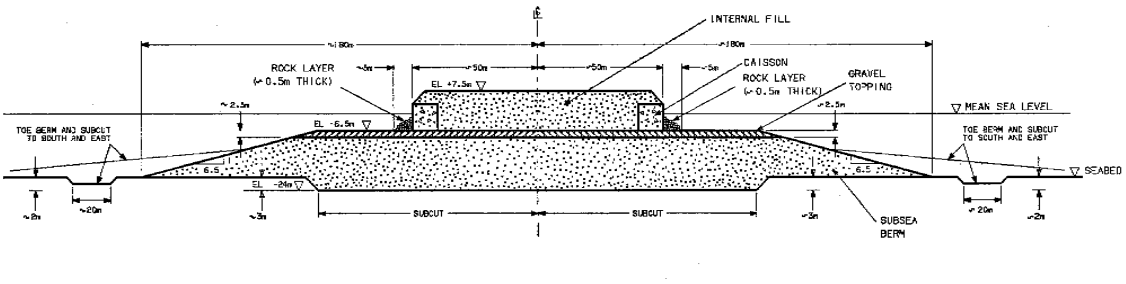

Figure 9: Side view through Tarsiut caisson structure

3.2 Instrumentation on the Tarsiut Structure

Instrumentation comprised sensors to measure loads on the outer face, strain gauges embedded in the concrete and geotechnical sensors in the foundation and core. The strain gauges were of a weldable type and were attached to the steel reinforcing rods in the concrete. Gauge locations were selected on the basis of finite element calculations that also provided calibration coefficients for converting the measured strains to ice loads. From the location of the gauges, it was possible to establish load distributions and global loads. In spite of the care taken in the installation of gauges and cables, only a third of the gauges were operational at the beginning of the measurement program. Fortunately there was sufficient redundancy that useful results could still be obtained. A system of four 4 m by 4 m flat jack panels was attached to the outside of the east caisson. The outer face of each panel was an 89 mm thick steel plate to ensure that applied ice loads were uniformly distributed to the 16 flat jacks behind each panel. Pressure transducers measured the flat jack pressures.

Circular load cells were mounted in 880 mm diameter recesses in the north caisson. The sensing face was supported on shear bars or spiral coil hydraulic hoses. For more details on the characteristics of these transducers see Graham et al. (1983). The shear bar transducers had a number of desirable features (low temperature coefficient, no creep and high stiffness). The spiral coil transducers had less desirable features but were inexpensive. Unfortunately a storm in the autumn led to water entering these gauges and making a number of them inoperable. Finally, eight 50-mm diameter microstud gauges were installed in one of the flat jack panels to measure local pressures. These were a diaphragm type of pressure gauge.

Experience over the winter of 1981-82 showed that the embedded strain gauges and flat jacks provided consistent and reasonable ice load information. Inclinometers provided qualitative confirmation of major ice loading events and quantitative information for operational purposes.

During the winter of 1982-83, there was no drilling activity on the structure but it was left in place and used as a research platform. The island was manned with approximately 6 to 10 people, and measurements of ice loads, ice failure behavior and ice movements were made. The ice load measurements were primarily obtained from the output of a large number of MEDOF panels[1] that were used to circle the structure (Figure 10). In addition, a few panels were placed further out in the grounded rubble field. During March to May, measurements were made by British Petroleum (BP) around the grounded rubble field (see Figure 11) to provide information on the local strain and strain rates in the adjacent ice sheet. Based on this information, the global loads on the island and rubble pile were inferred. A particular aspect of this work was the determination of the attenuation of loads through grounded rubble. In spite of the extensive work program, this question was not quantitatively answered.

[1] MEDOF panels, which are 1.1 x 2.7 m in area, are a total load type of panel, i.e. they sense the total ice load on them. The contact area of the ice on the panel has to be estimated in order to determine the effective ice pressure. The panels can be deployed in either vertical or horizontal arrays, which allows local load distributions and global loads to be determined. They are a sandwich of two steel plates (inner plate about 2 mm thick and the outer plate is about 10 mm thick) over an array of polymeric buttons. The panels are closed at the edges and filled with a calcium chloride solution. Load application to the panel causes the buttons to compress and the internal volume of the panel to change. This volume change causes the calcium chloride fluid level in a stand pipe attached to the panel to change. A sensitive pressure transducer is used to measure the hydrostatic head changes in the standpipe. The maximum frequency response is estimated to be about 1 Hz.

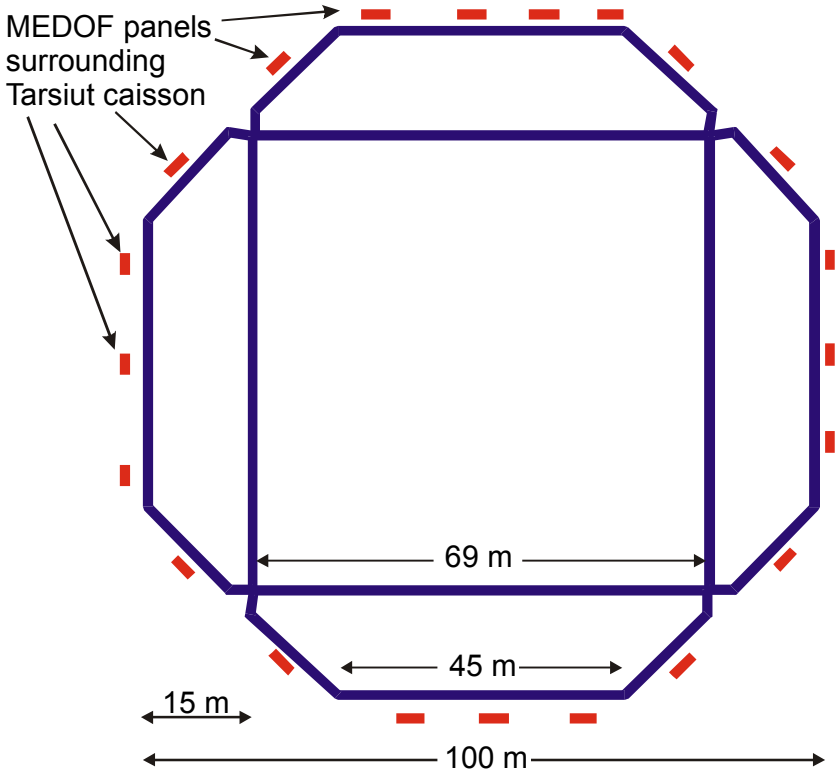

Figure 10: Illustration of MEDOF panel locations surrounding Tarsiut caisson during the 1982/83 season

3.3 Tarsiut Ice Loading Events

There were a number of different loading events defined for the 2 years that Tarsiut Island was deployed in the Beaufort Sea. The NRC Centre on Ice Loads (Timco 1996, 1998) has a complete set of reports that describe the measurement program and results. Although there were a number of different ice-loading events described in the reports, the information about them was not complete and often several assumptions were made in the calculation of the load. After reviewing the information, four ice-loading events were identified – one in 1981-82 and three from 1982-83. These are shown as a Line Load on the structure as a function of the ice thickness in Figure 12. In this approach, the measured global load has been normalized by the width of the structure being loaded by the ice. It should be noted that, although these were chosen as the best events, there was discrepancy in the estimated load by using different sensors and the time-series traces are very incomplete. The events are included since they represent the loads reported on the first wide offshore structure deployed in severe ice conditions.

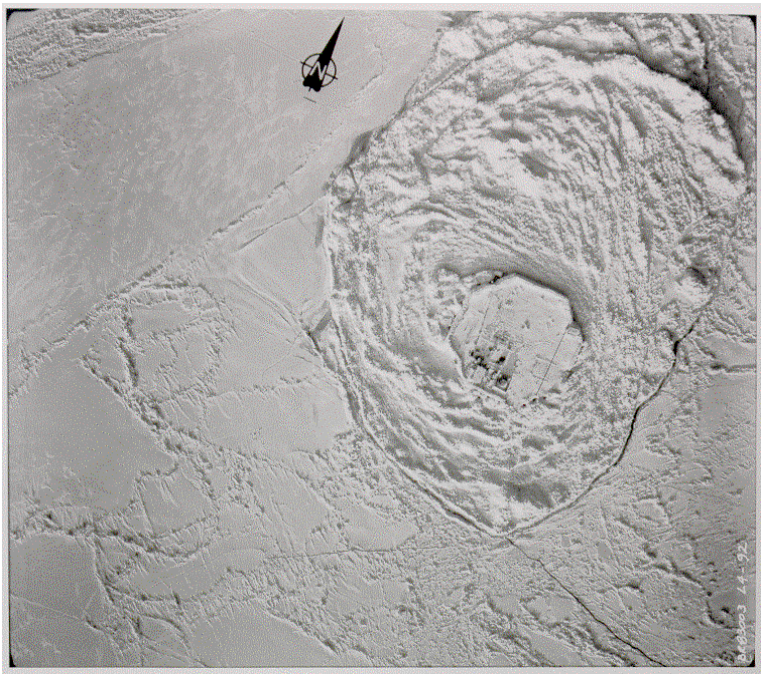

Figure 11: Overhead view of Tarsiut Caisson showing the grounded rubble field surrounding the structure (photo taken on March 2, 1983).

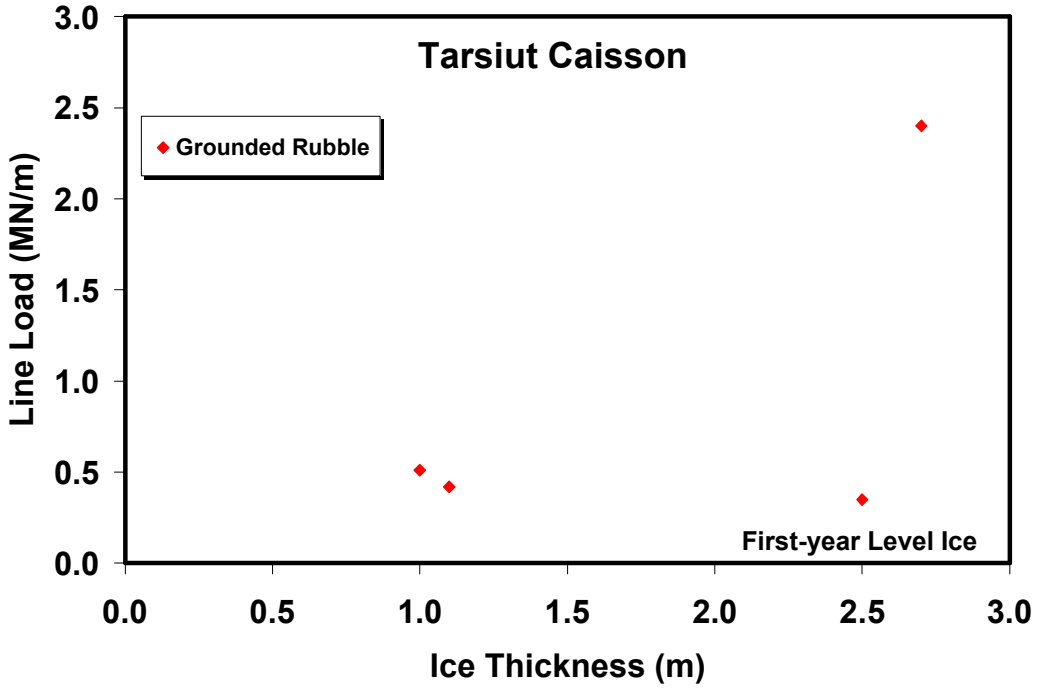

Figure 12: Line-Load on the Tarsiut Caisson as a function of ice thickness. Note that in all cases there was a 150 m grounded rubble field surrounding the structure.

4.0 SINGLE STEEL DRILLING CAISSON (SSDC)

4.1 Description of the SSDC

Canmar owned and operated the SSDC. This structure was a converted super tanker that had undergone extensive modifications to adapt it for use as a support structure for year-round exploratory drilling in the Beaufort Sea (Figure 13). The structure is 162 m long, 53 m wide, and 25 m high. All sides are vertical at the waterline. It was initially designed to rest in a water depth of 9 m. From 1982 to 1984, the SSDC was installed in the Canadian Beaufort Sea at the Uviluk and Kogyuk sites, where it rested on a submerged berm. In August 1986, the SSDC was modified in preparation for installations in the U.S. Beaufort Sea (1986-1988). Modification of the SSDC involved mating the drilling vessel to a semi-submersible steel base, the "MAT" (Figure 14). This steel base alleviated the need for a dredged berm, and gave it the capability to operate year-round in water depths of 7 to 24 m, and a wide variety of soil conditions. The SSDC was deployed with the MAT at the Phoenix, Aurora, Fireweed and Cabot sites in the US. Beaufort Sea. A sketch of the SSDC and MAT is shown in Figure 15.

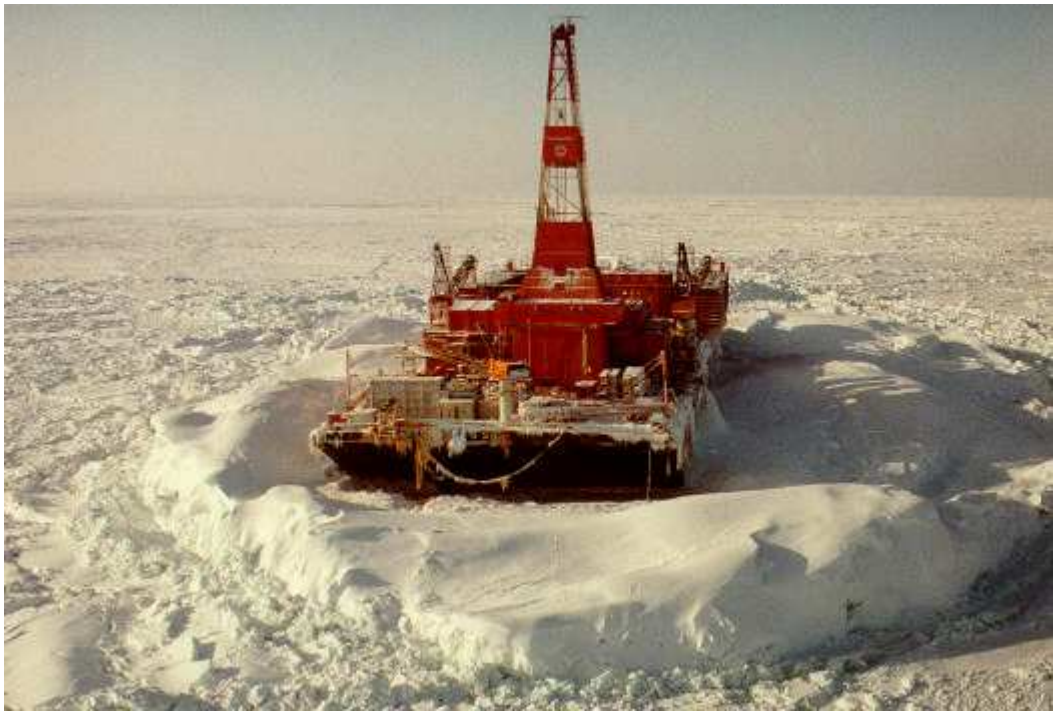

Figure 13: SSDC at the Kogyuk site in the Beaufort Sea. Note the sprayed ice rubble surrounding the structure.

Figure 14: Artist's cut-away illustration of the SSDC and the MAT.

4.2 SSDC Instrumentation and Ice Loads

The instrumentation was different at each of the drilling sites. The following discussion describes the instrumentation at four of the six installation sites in the Beaufort Sea (no information was available for the Fireweed and Cabot sites). Note that first two sites were in the Canadian Beaufort, whereas the later two sites were in the American Beaufort. The only sites that had reliable ice load measurements were the Alaskan sites (Phoenix and Aurora).

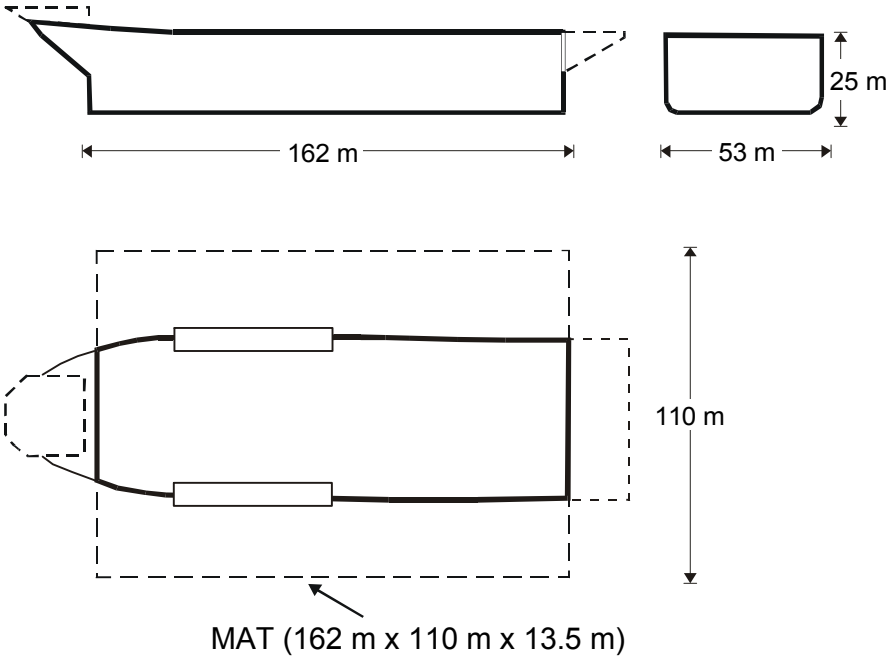

Figure 15: Dimensions of the SSDC and the MAT

4.2.1 Uviluk Site, 1982 – 83

During the summer of 1982, the SSDC was deployed in a water depth of 31 m on a sub-sea berm at the Uviluk P-66 location in the Beaufort Sea. At this site, the hull was instrumented with three types of load panels: MEDOF panels, Arctec pressure panels and Weir Jones fluid filled panels (see Figure 16). The MEDOF panels (1 m x 2 m) were welded in pairs (at waterline) on all sides of the hull. The Arctec shear bar panels were arranged in a vertical array near the starboard midship. A total of 13 discrete panels with sensor areas 0.5 m x 0.5 m, 1 m x 1 m and 1 m x 2 m were welded to the vessel at this location. A total of 8 Weir Jones panels were located at the waterline on the bow of the SSDC. These units contained rectangular flatjacks (4.1 m x 2.0 m) filled with hydraulic fluid. MEDOF panels were also installed *in-situ* at the outer edge of the ice-berm.

A grounded rubble pile surrounded the SSDC at the Uviluk site (Figure 13) so there was no direct ice-structure interaction except during the early part of the season.

At the Uviluk site, the threshold for the instrumentation was set high in anticipation of high ice loads. However, the formation of the grounded rubble field effectively shielded the structure and the applied ice loads were below the detectable limit of the instrumentation. As a result, there are no time-series traces for the three interactions with level first year ice that occurred at Uviluk so there are no recorded ice load events from this site.

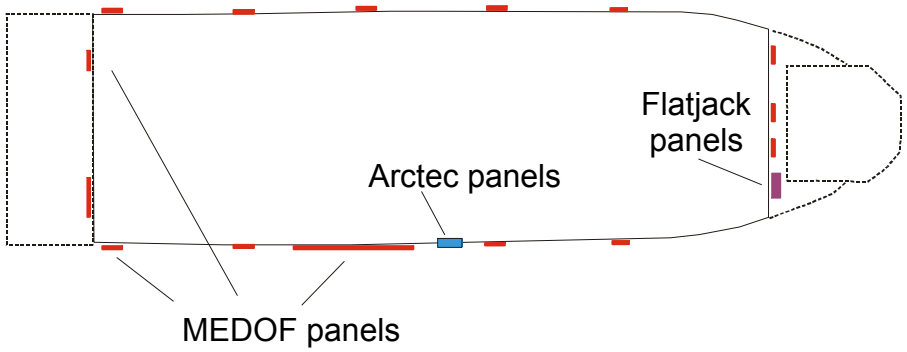

Figure 16: Location of the load measuring sensors on the SSDC at the Uviluk site.

4.2.2 Kogyuk Site, 1983 – 84

During the 1983-84 season, CANMAR operated the SSDC for Gulf Canada Resources Ltd. to drill an exploratory well at the Kogyuk N-67 site, in a water depth of 28 m. The SSDC was set-down on a submarine berm that was reduced in size from the original design specifications (Hewitt et al., 1985). The three types of ice load panels installed on the SSDC while it was deployed at Uviluk (see Figure 16) were functioning at the Kogyuk site. However, at the Kogyuk site, no *in-situ* MEDOF panels were installed in

the surrounding ice. Hull gap LVDTs, ice pad sensors and ice reflectors (for monitoring ice movement) were positioned at specified locations in the ice.

Similar to the Uviluk site, a grounded rubble field effectively shielded the structure at the Kogyuk site.

The SSDC experienced 11 interactions at the Kogyuk site involving first year, second year and multiyear ice (Canmar, 1985). No load-time series are available for those 11 reported interactions. The most notable events were two impact events that occurred on September 25, 1983 and at break up, in June 1984 (Hewitt, personal communication).

The September 25 Event occurred shortly after set down of the SSDC, while the effective ballast was estimated to be only 300 MN. A large multiyear ice floe impacted the port bow of the SSDC. The floe diameter was estimated to be 1.7 km, and the ice thickness was estimated as 3 to 4 m. The speed of the impact was estimated to be 0.25 m/s. The ice floe penetrated about eight meters, failed in pure crushing (without splitting or bending) and came to a halt. Although the impact was clearly felt, no damage or movement of the SSDC was detected. The SSDC resistance at the time of impact was estimated to be about 175 MN (Hewitt et al., 1985). Based upon this estimate and estimates of the floe mass and deceleration, Canmar estimated that the load was less than 100 MN (Hewitt, personal communication).

On June 25, 1984, a second-year floe impacted the stern of the SSDC at an estimated speed of 0.45 m/s. The floe size was estimated to be 24 by 13 km with a thickness of 1.5 to 2 m. A grounded ice rubble feature at the stern may have shielded the hull from direct contact during most of the event. The MEDOF panels registered a response to this impact, from which a load of less than 100 MN was estimated (Hewitt, personal communication).

4.2.3 Phoenix Site, 1986 – 87

In September 1986, the SSDC/MAT was deployed at the Phoenix site in Harrison Bay, Alaska, at a water depth of 17.5 m. Since the waterline was 4 m above the top of the MAT, direct ice interactions with the flat sides of the SSDC occurred.

The ice load panels installed on the hull of the SSDC while deployed at Uviluk and Kogyuk were not functioning at the Phoenix site. Instead, load panels were placed in the ice and used to monitor the ice loads. In early March 1987 four IDEAL ice force panels (0.5 m by 2.0 m) were installed in the rubbled ice surrounding the SSDC on the north side, and six additional load panels were located in the level first year ice, as shown in Figure 17. Ice loads were measured continuously from installation of the panels in March to their removal in June, 1987. In addition, the ice conditions at Phoenix were monitored via ice movement reflectors, crack displacement stations and thermistor strings. Information about the ice was also provided by aerial photography, ice rubble profiles, ice thickness, ice salinity measurements and ice observations (Blanchet and Keinonen, 1988).

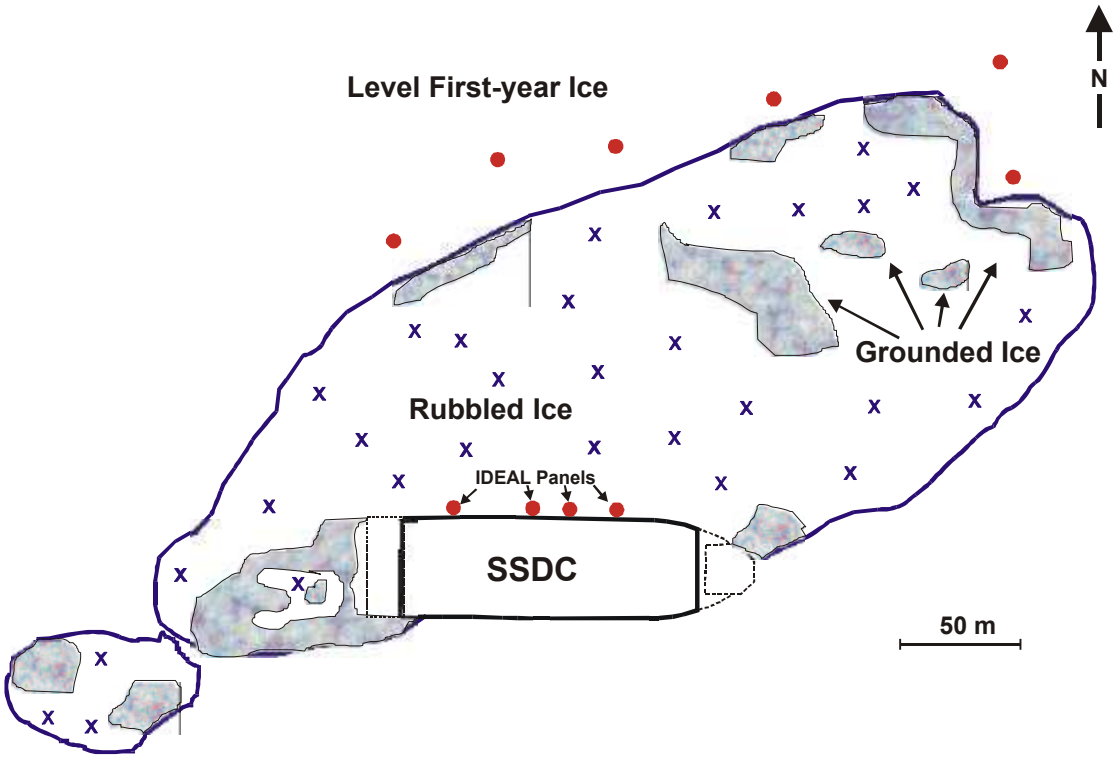

Figure 17: Location of instrumentation in the ice surrounding the SSDC/MAT at the Phoenix site (1986-87).

The load panels were scanned at a rate of 20 Hz. The data were stored in a temporary buffer and the 1.5-minute average of each panel was subsequently computed. These averages were stored in a daily buffer that was recorded onto a daily disk every 24 hours. The analysis of the SSDC and its applied loads were derived from a 1.5 minute average of the panel results. Blanchet and Keinonen (1988) calculated the total load on each side of the SSDC using

$$L_{SSDC} = \frac{L_{Ideal} \; x \, C_{incl} \; x \, C_{thick} \; x \, C_{scale} \; x \, W_{SSDC}}{w_p} \qquad (1)$$

where
L_{SSDC} = hourly average of load on impacted face
L_{Ideal} = maximum hourly average ice load measured by the affected panel
C_{incl} = inclusion/cross-sensitivity coefficient
C_{thick} = through thickness coefficient
C_{scale} = scale coefficient
W_{SSDC} = width of impacted face 162 m - starboard
52 m - stern
38 m - bow
w_p = 0.5 m panel width

The coefficient, C_{incl}, was introduced to account for the inclusion and cross sensitivity effects associated with the load panels[2]. Cross sensitivity effects, which result from the simultaneous application of lateral and normal loads to the panel, can also produce increased estimates of the applied load. The combined effects of inclusion and cross-sensitivity during creep can account for an increase in load that can be represented by a load ratio of about 1.25, or C_{incl} of 0.8 (Blanchet and Keinonen, 1988).

The C_{thick} coefficient was introduced to take into account the completeness of load measurement of the 2 m long panel measuring the applied load throughout the full thickness of the ice. Since the ice thickness differs according to the particular Event, C_{thick} also varies.

The C_{scale} coefficient was introduced to account for any "scale effects" during an ice-structure interaction. During creep loading, it was assumed that there was no scale effect. Hence, C_{scale}, was taken to be unity in the calculation of the load (Blanchet and Keinonen, 1988).

While the SSDC was at Phoenix, the landfast ice became unstable on January 30 and moved about 500 m from the northeast, creating grounded ice rubble (Figure 18). This rubble field remained stable for the rest of the winter (Blanchet and Keinonen, 1988). After the formation of the port side ice rubble on January 31, the ice around the SSDC/MAT became immobile. The 500-m long wake refroze on the starboard side and beyond the stern rubble. Although periods of high winds occurred before break-up, no significant movements of the landfast ice were measured. The landfast ice did experience a cyclical motion due to wind, thermal or tidal stresses. The decay of the rubble began at the end of May. The surface of the ice melted at low areas within the rubble and the level ice. Water accumulated on top of the ice until it was able to drain through holes in the ice.

There were six notable ice-structure interaction events between March and June, 1987. Each of the interactions occurred when the surrounding landfast, rubbled ice encroached upon the port side of the SSDC, due to thermal and wind-driven stresses. Global loads were derived from the response of the four load panels along the port side of the SSDC (see Figure 17). The global load associated with those six interactions ranged from 25 Mn to 74 MN.

[2] Studies have shown that the stress field in the ice is disturbed when objects are introduced in to the ice (see e.g. Croasdale and Frederking 1986). As a result, the response registered by the load panels can be different than stresses measured in ice. This artifact of the load panels is produced by the difference in stiffness between the load panel and the surrounding ice. The load panel affects the local stress distribution in the ice and introduces a 'hard spot'.

Figure 18: Photograph of the SSDC at the Phoenix site. Note the large rubble field surrounding the structure.

4.2.4 Aurora Site, 1987 - 88

In 1988, the SSDC/MAT was deployed at the Aurora site in a water depth of 21 m. At this site, ten *in-situ* load panels monitored the applied load adjacent to the hull of the SSDC as well as the load applied in the region outside the rubble ice (Figure 19). Five of the panels were located in the rubble off the bow. Two other panels were installed at starboard, and three panels were installed in rubble near the stern. Due to the large amount of broken ice and the instability of the ice to the north of the SSDC, no *in-situ* ice load panels were installed on the port side of the SSDC. Ice conditions surrounding the SSDC were monitored through crack displacement stations, thermistor strings, ice movement reflectors, wire line devices. Numerous boreholes were used to measure ice thickness and determine the profile of the underside of the rubble (Blanchet and Wiefelspuett, 1988).

Ice conditions at the Aurora site were more dynamic than at the other sites. The SSDC was bounded on the south by landfast ice that had stabilized by the end of November, 1987. The ice to the north, east and west of the SSDC was more mobile. Borehole drilling indicated that the rubble in all sectors was floating. Rubble formations near the bow stern and starboard stern corners had sail heights that ranged from 2 to 3 m, with individual blocks up to 4 m high. The enclosed flat pans consisted of single or rafted layers of level ice. The ice in contact with the starboard side of the SSDC was mainly level ice, with isolated rafted areas and some rubble that extended less than 1 m from the hull.

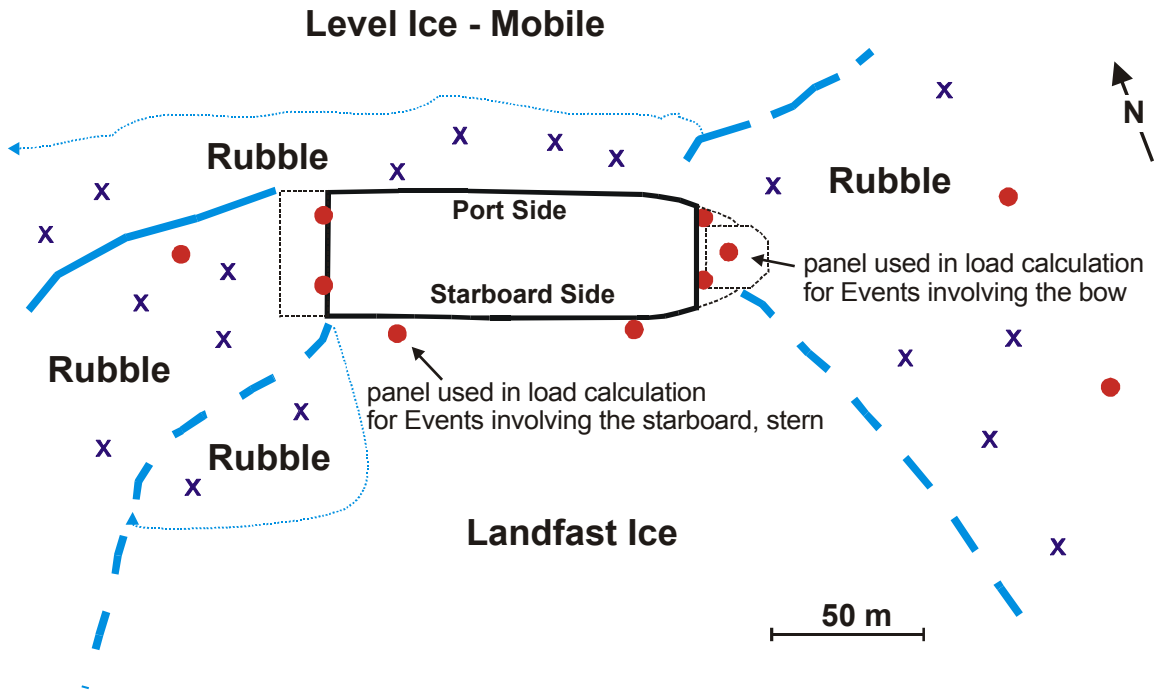

Figure 19: Location of instrumentation in the ice surrounding the SSDC/MAT at the Aurora site (1987-88).

During the project period, the average level ice thickness surrounding the SSDC increased from 1.22 m to 1.55 m, with a maximum of 1.58 m on June 1, 1988. The growth of the consolidated layers at both the bow and stern locations were estimated to be from 2.2 m in March to 3.5 m in June for the bow ice, and from 1.7 m in March to 3.0 m in June for the stern ice.

Ice adjacent to the SSDC developed cracks that extended 45° from the centerline of the SSDC, and divided the surrounding ice into four regions classified as the *bow, starboard, stern* and *port* sectors (Figure 19). Ice at the *bow, stern* and *port* side of the structure moved with the predominant wind direction, which was generally in the east-west direction[3]. Ice in the *port* sector remained unstable throughout winter until breakup, with daily movement from 0 to 20 m. The ice sheet in the *starboard* section had a cyclical motion between the shoreline and structure (normal to the longitudinal axis) that was wind and temperature driven.

The ice loads at the Aurora site were determined using the same methodology as that at the Phoenix site. Nine loading events occurred between March and June, 1988, seven of

[3] The ice movement direction was consistently 30° to 60° to the right of the wind direction. At Aurora, 54% of winds were from the ENE direction and 30% of the winds were from WSW direction. All winds greater than 16 m/s were from E or ENE for all but one day (February 21, 1988).

which were analyzed. These events resulted from wind/thermally driven stresses and involved the bow and starboard sides of the vessel. Load estimates for interactions involving the bow were obtained from the *in-situ* load panel located towards the centre of the bow. The two surrounding panels on the bow were damaged during the second ice-bow interaction of that season. Global load estimates for the event that involved the starboard side of the vessel were obtained from the *in-situ* panel located on the starboard side, near the stern. The load occurrences at Aurora were classified as pure creep interactions, or a combined failure mode of creep and "racheting".

4.2.5 Overview of Ice Loads on the SSDC

Figure 20 shows a plot of the Line Load as a function of the ice thickness for all of the events in which load information was available (Phoenix and Aurora sites). Note that for all of these events, a rubble field surrounded the SSDC. The data in the plot have been subdivided according to the state of the rubble surrounding the SSDC. Although the rubble fields were mostly floating, there were grounded regions close to the SSDC at the Phoenix site.

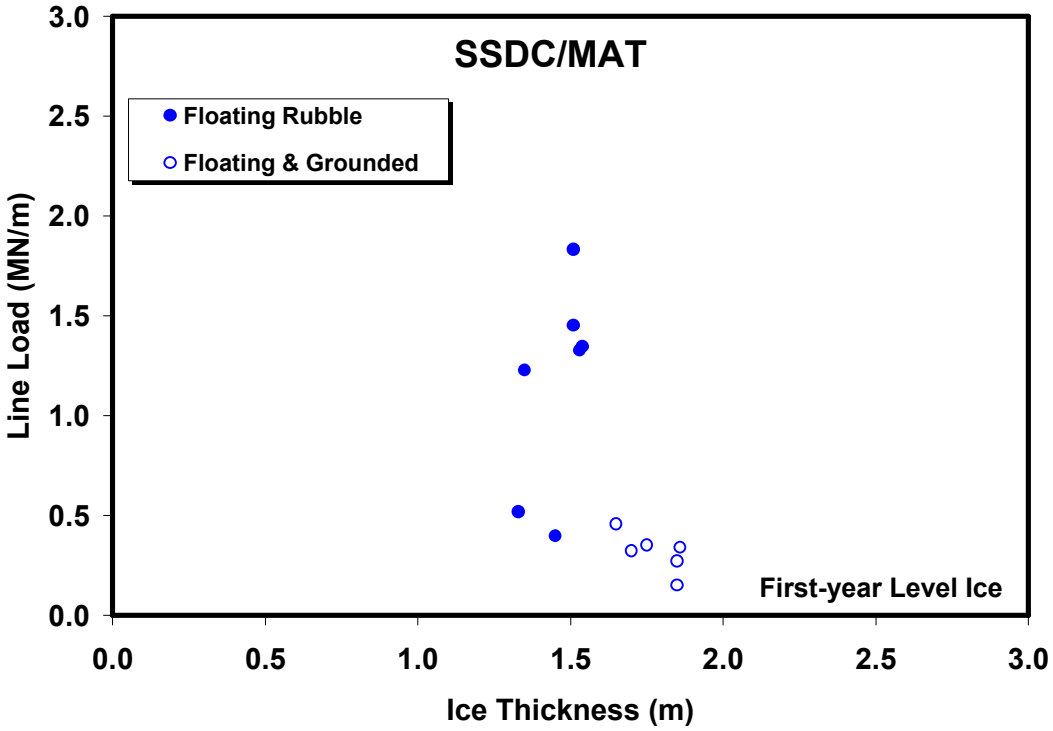

Figure 20: Line Load on the SSDC as a function of the ice thickness.

5.0 CAISSON-RETAINED ISLAND (CRI)

5.1 Description of the CRI

Esso Resources Canada Ltd. originally built this structure, but it is now owned by Arctic Transportation Ltd. It was developed as a means of reducing dredge quantities, as compared to the more traditional sand island. The CRI was built in 1982-83 and first deployed in the Canadian Beaufort Sea in the summer of 1983. The design has 8 individual caissons (43 m long x 12.2 m high x 13.1 m wide) in a ring (see Figure 21). Two pre-stressed bands of steel wire cable hold the caissons together. The central core, which is 92 m across, is filled with sand to provide a surface for drilling operations and to provide stability against applied loads. The CRI is an 8-segment octagonal-shaped steel structure about 118 m across on the flats, 12 m high and the outer face is inclined (30° from the vertical).

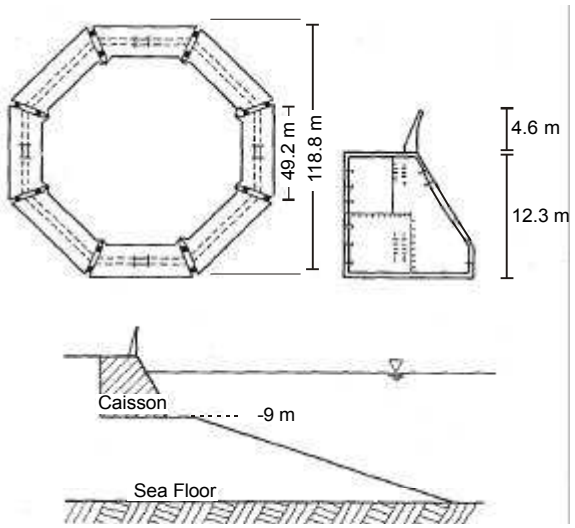

Figure 21: Illustration of the Caisson Retained Island (after Croasdale, 1985)

The CRI was deployed for three seasons in the Canadian Beaufort Sea:

1. From September 1983 to April 1984 it was deployed at the *Kadluk O-07* in Mackenzie Bay site at a water depth of 14.5 m. A spray ice island was constructed to the north of the CRI to provide an emergency relief well drill site.
2. In August 1984 the CRI was moved to the *Amerk O-09* site where it remained until March 1985.
3. From October 1986 to January 1987, the CRI was deployed at the *Kaubvik I-43* site.

5.2 Hull Instrumentation on the CRI

Instrumentation on the CRI consisted of sensors for ice loads on the outer surface of the caisson, strain gauges on structural elements of the caisson and geotechnical sensors in the sand core and under the foundation (Hawkins et al., 1983). A schematic of the layout

of the sensors is shown in Figure 22. The majority of the load sensors were installed on the north, northeast and northwest caissons, to provide coverage to the faces over the anticipated, predominant direction of ice movement. Ice force sensors on the outer surface comprised three different sizes and types:

1. The microcells, which had a diameter of 165 mm, were the smallest sensor. They were a temperature-compensated, strain-gauged diaphragm-type of sensor. Four clusters of 4 sensors were flush-mounted on the north quadrant of the caisson at the waterline, and several more pairs were mounted on the adjacent faces (Figure 22). They measured point (or local) ice loads and had a high load capacity of 35 MPa and a short response time.
2. The maxicell, which had a diameter of 815 mm, was a sensor that measured pressure in a spiral coiled hydraulic tube sandwiched between two steel plates. It was, effectively, a load cell with an equivalent capacity of 7 MPa. Because of its construction it did not have a short response time. A total of 8 of these sensors were mounted on the southern half of the caisson. They were supported by structural stringers and were flush with the surface. During their first year of operation, the maxicells proved to be unreliable. They were subsequently replaced by a pair of microcells, which were mounted on an adapter plate (Croasdale et al., 1988).
3. The third type of sensor was a shear bar-type with a load sensing surface 2.1 m high by 0.5 m wide. Strain gauged shear bars sensed the normal component of the ice load applied to them. They had a full-scale range of about 3 MPa. Nine of these sensors were deployed around the northern half of the caisson.

The internal structure of the caissons was also instrumented with 156 weldable strain gauges. The locations were determined from a finite element analysis that also provided a means for interpreting ice loads from the measured strains. Geotechnical sensors were used to measure the response between the caisson and the sand and foundation. This instrumentation included total pressure cells, pore pressure cells and inclinometers. The instrumentation was sampled at a frequency of either 0.1 Hz or 1 Hz. To reduce the quantity of stored data, real-time data processing techniques were used. This involved storing the average, variance and peak reading for each sensor over a five-minute interval.

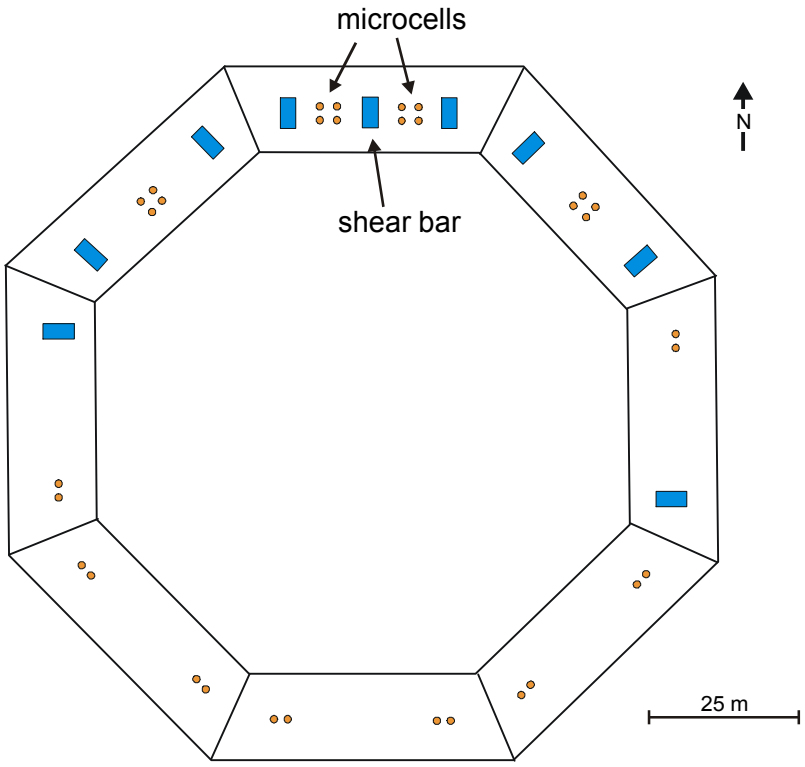

Figure 22: Illustration of the location of the instrumentation on the hull of the CRI.

5.3 Field Instrumentation and Ice Loads on the CRI

In addition to the hull instrumentation, a number of different sensors were placed in the ice surrounding the CRI. In the following sections the ice conditions, field instrumentation, and measured loads are described for each of the three sites.

5.3.1 Kadluk, 1983-84

When the CRI was deployed at Kadluk in 1983-84, early ice movement was restricted by grounded second-year ice, and an ice rubble field did not form. A later movement of the landfast ice allowed ice about 1.0 m thick to interact, directly, with the caissons. By the first week of March, the surrounding first year sea ice was about 1.7 m thick, and there was an extensive grounded rubble field on the southwest side of the CRI. A few small grounded multiyear floes were observed to the east and north of the CRI (Johnson et al., 1985). On March 11, strong southerly winds caused ice on the north side of the CRI to break away and move out to sea, which left the CRI-ice island-rubble area as a peninsula on the edge of the inshore flat ice.

During the spring of 1984, 18 cylindrical, biaxial ice stress sensors[4] were installed in the level ice south of the CRI, beyond the rubble (Cox, 1987). Due to complications, the *in-situ* sensors were not finally positioned until the first week of April. Since ice north of the CRI remained thin and continued to move offshore at that time, the sensors were deployed at six sites south of the island (on the shoreward side, Figure 23). At each of the six sites, the sensors were located at ice depths 0.3 m, 0.8 m and 1.3 m. An Exxon pressure panel was installed on the south side of the structure, about 20 m from Site 2, with the panel facing 6° from north. In addition, the ice temperature, ice movement and wind speed and direction were monitored.

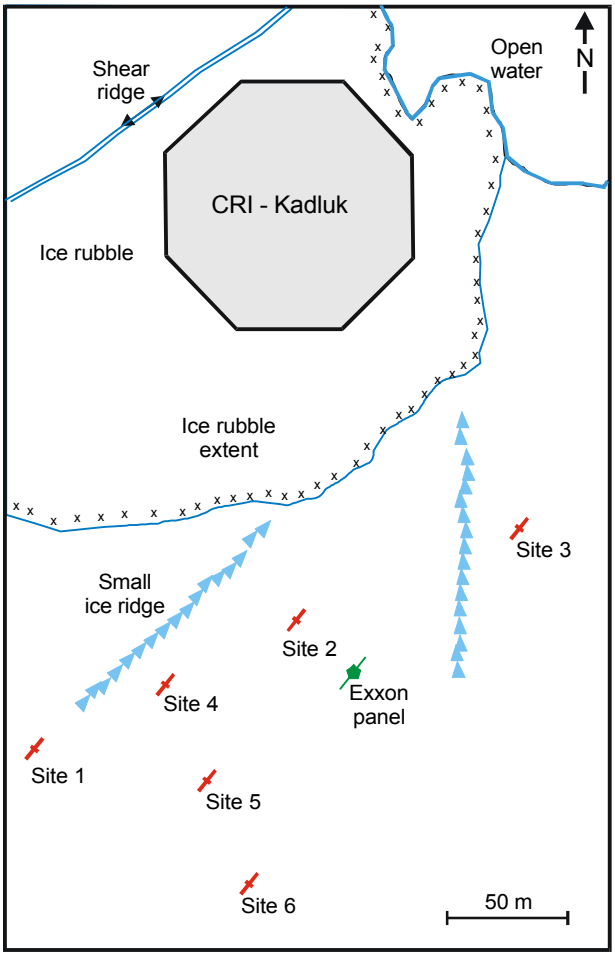

Figure 23: Ice conditions and instrumentation at Kadluk, spring 1984 (after Johnson et al., 1985 with adaptations).

[4] The biaxial stress sensor consists of a stiff, steel cylinder that allows the principal ice stresses normal to the axis of the gauge to be determined by measuring the radial deformation of the cylinder in three directions (using vibrating wire technology). The sensor itself is 20.3 cm long, 5.7 cm in diameter and has a wall thickness of 1.6 cm. The biaxial stress sensors have been used to measure thermal stresses in New Hampshire lakes (Cox, 1984) and ice forces on Adams Island (Frederking et al., 1984).

Johnson et al. (1985) noted that when the ice was not subjected to any appreciable load, the principle stress direction varied with depth. However, when the panel stress exceeded 100 kPa, the principle stress directions became aligned in the top, middle and bottom of the ice sheet. Stresses at all depths had a diurnal variation in response to air and ice temperatures. The complexity of the ice stress distribution versus depth was attributed to the occurrence of bending failure of the level ice (observed along the length of the rubble pile in front of the structure), with contributions from thermal stresses in the ice sheet. Lateral variations in the stress at any given level were also complex. However, in general, the average full thickness ice stress did appear to increase from west to east along the measurement line. This was attributed to the presence of grounded multiyear ice at the east end of the line of the sensors (Johnson et al., 1985). During inactive periods the ice did not show the lateral increase in stress from west to east.

No time-series traces are available for the global load on the CRI at Kadluk. However, Johnson et al. (1985) computed the total load from the average normal and shear stress measurements at Sites 1, 2, 3 and 4 and summing them across the ice peninsula. They state that the total ice load on the CRI-rubble complex at Kadluk during April and May was thermally induced. The peak structural load associated with the thermal activity of the ice was estimated to be about 150 MN. In their analysis, Johnson et al. (1985) did not account for the influence of ice rubble on the magnitude of structural loads.

5.3.2 Amerk, 1984-85

In 1984-85 the CRI was located at Amerk, where it was surrounded by grounded rubble (Figure 24). As such, the grounded rubble transmitted ice loads to the underwater berm and the caissons experienced negligible load (Croasdale, 1985). In general, the rubble had a sail height from 0 to 4 m above sea level, although the northeast part of the rubble field had sails that approached 10 m in height (Sayed et al., 1986).

In March 1985, *in-situ* ice sensors were installed in the rubbled ice surrounding the CRI. Since the floating ice was expected to move in a predominantly westward direction and thermal stresses/expansion would be applied relative to the nearest shoreline, the east and south sectors of the rubble field were monitored for ice pressure and movement (Sayed et al., 1986). Various types of instrumentation were installed in the rubbled ice, including two Exxon Production Research (EPR) panels, three HEXPACK panels, an Ideal panel and a biaxial Canada Marine Engineering sensor (CMEL-IV) (Figure 25). The *in-situ* instruments were recorded at five-minute intervals. Ice movement records supplemented this information. The ice displacement was determined from a system of survey reflectors that were used in conjunction with an electronic distance measuring (EDM) instrument and a theodolite. Wind and temperature data also were recorded at the site.

Figure 24: Ice rubble surrounding the CRI at the Amerk site.

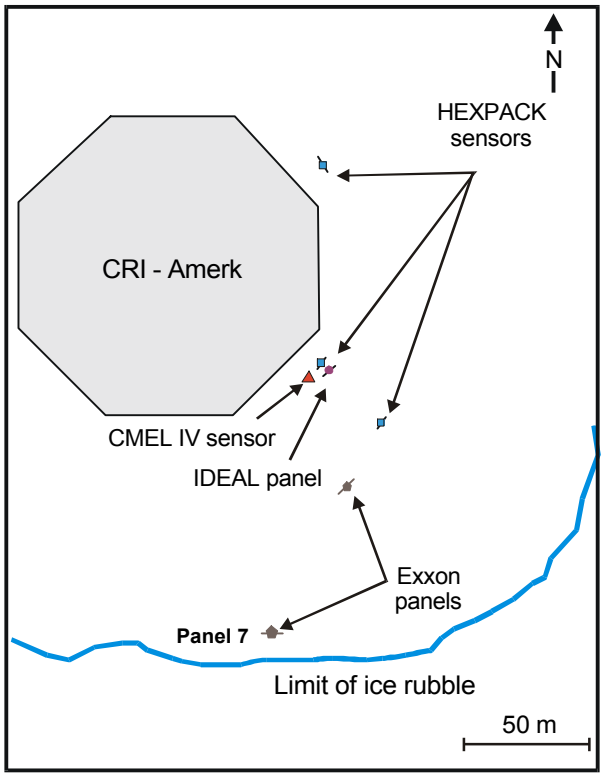

Figure 25: Instrumentation around the CRI at the Amerk site.

When the CRI was deployed at Amerk, over the winter of 1985-86, only the Exxon panel along the southern edge of the rubble (panel 7 in Figure 25) yielded appreciable results. All other sensors installed in the ice around the CRI showed no response. The stress-time trace for panel 7 is presented in Figure 26. During the period of instrumentation (March to May), the panel showed heightened activity during April 1 to 7, and then again beginning on April 22, 1985. During that period, the thickness of the refrozen rubble layer was 2.5 m. Sayed et al. (1986) estimated the load per unit length to be 500 kN/m, assuming the stresses were uniform across the frozen rubble. Since negligible stresses were measured near the caisson, it was concluded that the presence of grounded rubble resulted in significant attenuation of the applied load at Amerk (Sayed et al., 1986).

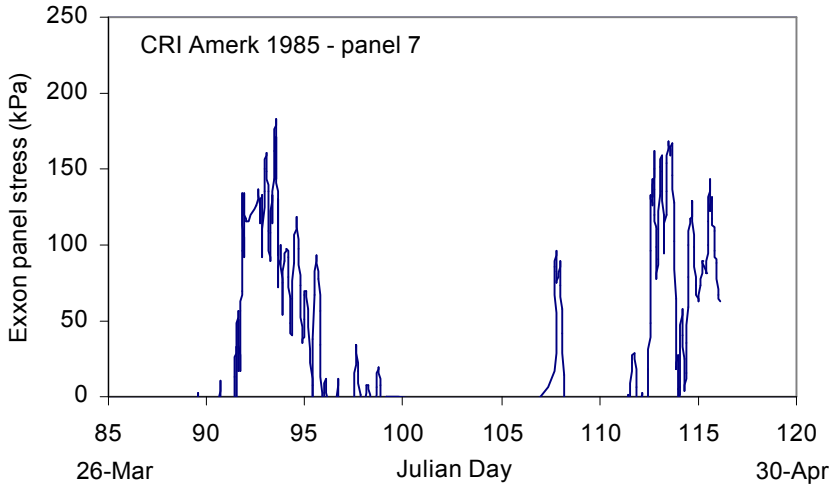

Figure 26: Stress measured on Panel 7 at the Amerk site from Julian Day 85 (March 26) to Julian Day 120 (April 30), 1985 (after Sayed et al., 1986 with adaptations)

5.3.3 Kaubvik, 1986-87

During the winter of 1986-87, the CRI was at the Kaubvik site. Moving pack ice surrounded it, and thin first year ice acted directly upon the caissons. In January, rubble began to develop around the structure. By February, a grounded rubble field surrounded the caisson, and remained stable until May (Figure 27). The thickness of the consolidated layer in most areas was about 2.5 m (below water level), and it was slightly thicker under rubble sails (Frederking and Sayed, 1988).

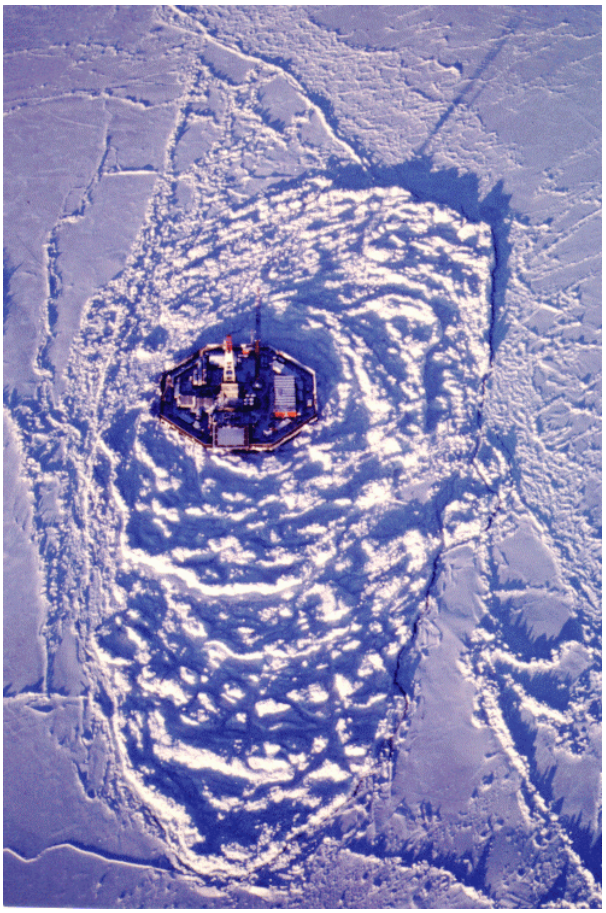

Figure 27: Photograph of the grounded rubble field around the CRI at the Kaubvik site.

A joint measurement program was carried out at the Kaubvik site with participation from Esso Resources Ltd, Memorial University of Newfoundland and the National Research Council of Canada (Croasdale et al., 1988). Esso Resources measured and recorded ice pressures on the caissons of the CRI and monitored the geotechnical behaviour of the foundation. Memorial University determined the strength and strain characteristics of the ice rubble and measured ice pressures and strains in the level ice surrounding the grounded rubble. The NRC measured the internal ice pressures, and the movements and profiles of the grounded rubble.

Four types of stress sensors were used to monitor the *in-situ* pressures in the ice rubble. The sensors were placed along radial lines extending away from the CRI, in order to measure the lateral stress profile of the load transmitted through the rubble field (see Figure 28). Three Exxon panels were oriented south-east of the caisson, extending to the outer edge of the rubble, where they would experience the effect of thermal expansion of the ice.

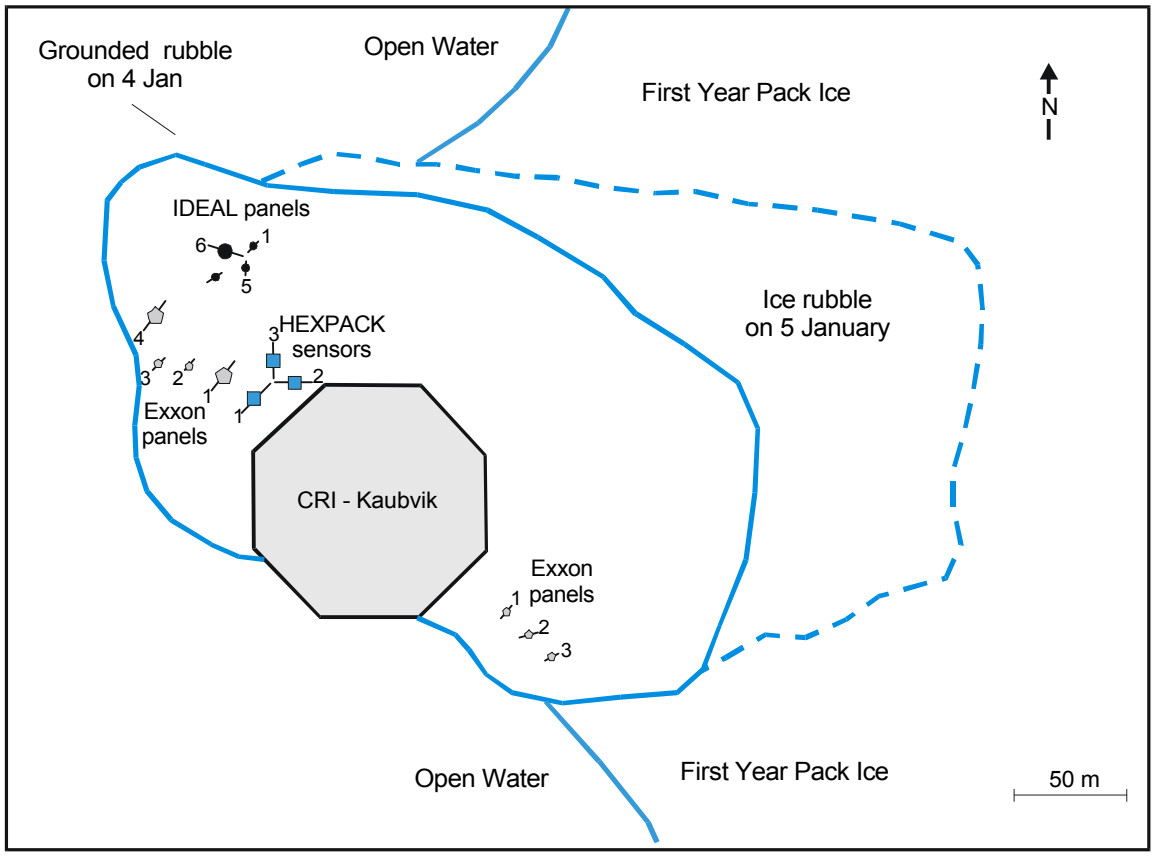

Figure 28: Location of the in-situ stress sensors in the rubble field surrounding the CRI at the Kaubvik site.

Since most storms approached from the northwest, the ice shear zone would be driven towards the CRI from this direction. Therefore, the majority of *in-situ* load panels were installed northwest of the CRI. The instrumentation included a radial line of four Exxon panels (0.5 m x 2 m), a rosette of three 1 m x 1 m IDEAL panels, a 1 m x 2 m panel and a rosette of circular HEXPACK panels (0.46 m diameter). The Exxon panels, IDEAL panels and HEXPACK panels were scanned and recorded at respectively 10, 15 and 30 minute intervals.

Ice movement was determined from an array of prism reflectors used in conjunction with an electronic distance measuring (EDM) instrument and a theodolite. Rubble surface profiles were taken along approximately radial lines from the CRI.

Memorial University installed three rosettes of BP-type sensors (mercury-filled, 75 mm diameter) in March, 1987 to monitor the late winter *in-situ* ice pressures associated with the level ice. By March, growth of the rubble field had stabilized. Therefore, the BP-type sensors were installed in the level, landfast ice, about 50 m southeast of the grounded rubble, at a depth of 0.6 m (Marshall, 1990, see Figure 29). The rosettes were arranged

so that one sensor in each rosette recorded the stress towards a given survey point on the southeast caisson of the CRI. The data were scanned and recorded every 2 minutes.

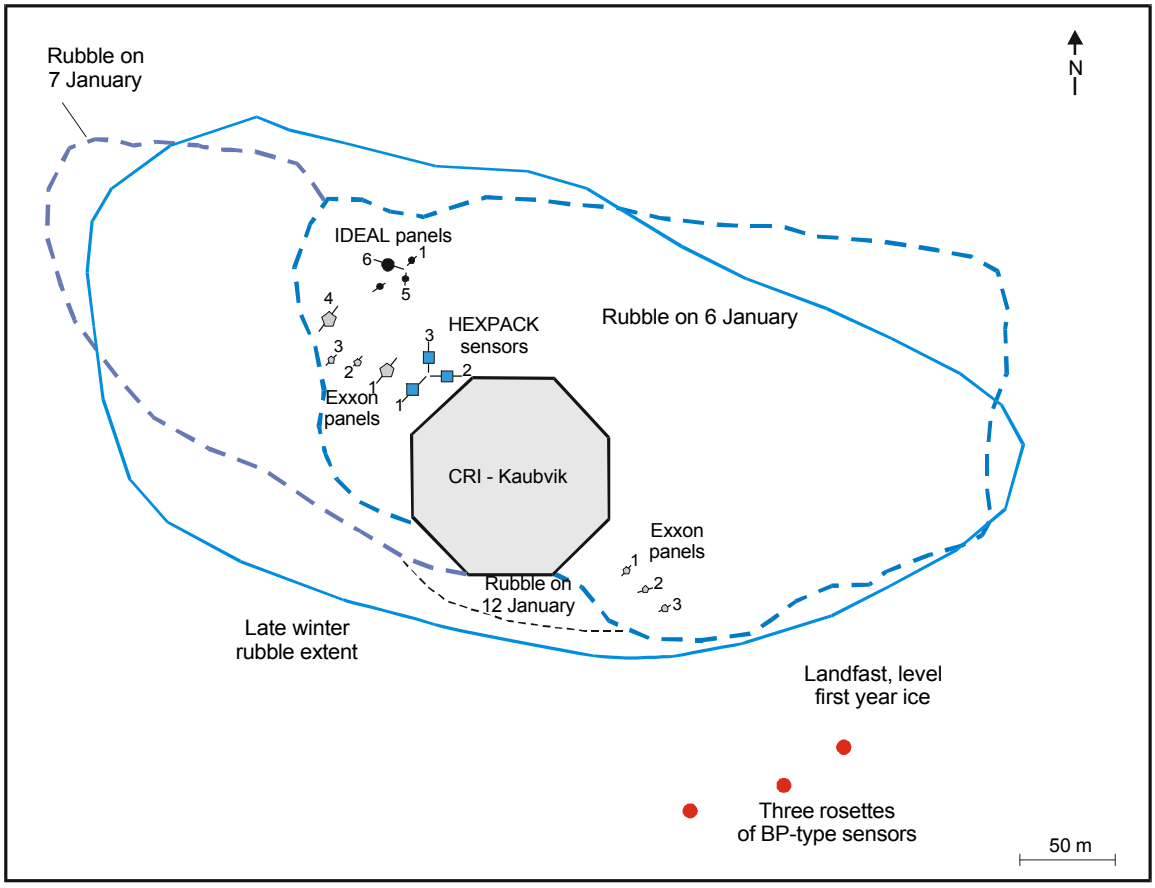

Figure 29: Late winter map of rubble extent around the CRI-Kaubvik showing location of BP-type sensors (after Frederking and Sayed, 1988; Marshall, 1990; with adaptations).

During the early winter period of 1987, the CRI at Kaubvik was directly exposed to advancing ice. However, the hull-mounted sensors showed that the early winter ice-structure interactions generated low ice forces, typically global loads of the order of 10 MN (Croasdale et al., 1988).

As the winter progressed, an extensive rubble field developed around the CRI at Kaubvik. The ice load panels that were installed in the rubble measured the *in-situ* ice stress (Figure 30). During the January 1987 field trip to Kaubvik, field personnel noted the occurrence of two rubble building events, one on the east side on the evening of January 5, and the other on the north-west side on the evening of January 7. The load panels registered a response to the January 7 event, at which time the rubble extent was in the vicinity of Exxon panels 3 and 4. Exxon panels 1 and 4 showed that the stress increased over a period of 2.5 hours, whereas Exxon panel 2 increased only slightly and

Exxon panel 3 first decreased and then increased to spuriously high values (Frederking et al., 1988). Figure 30 presents the output of panels 1 and 4 for this event, which are indistinguishable due to the temporal compression of the plot.

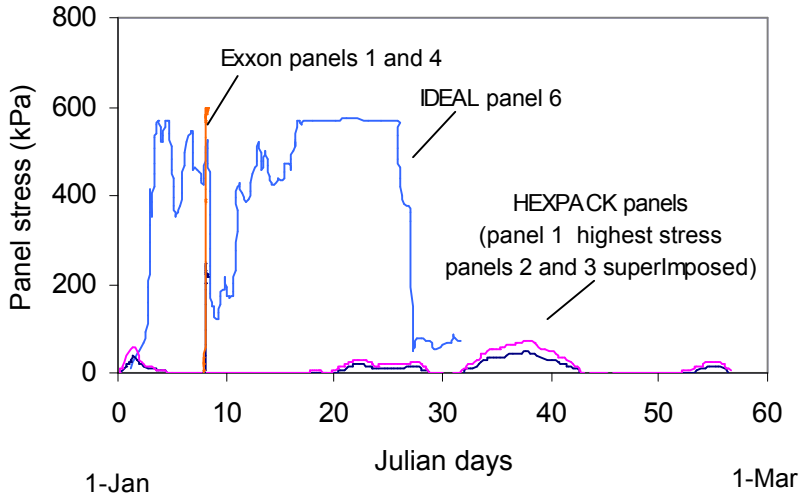

Figure 30: Output from the *in-situ* load panels installed around the CRI at Kaubvik (after Frederking and Sayed, 1988 with adaptations).

IDEAL panel 1 was initially relatively inactive and became more active from February 18 to March 8, where it showed a maximum stress of 350 kPa. IDEAL panel 6 (see Figure 30) showed a maximum pressure of about 500 kPa that occurred on January 27 and April 29 (not shown in the figure). In comparison, IDEAL panel 1, which was also active at that time, registered a peak pressure of 32 kPa (also not shown in the figure). The load registered by both panels was detected by the lower sections; the upper sections did not register load.

The rosette of HEXPACK panels recorded almost equal values of the normal stress in the three directions. The stress was approximately hydrostatic (Frederking et al., 1988). The output of the three HEXPACK panels is shown in Figure 30.

In the late spring, the output from the BP-TYPE sensors that were installed by Memorial University in the level ice to the south of the CRI (see Figure 29) indicated two events. The Exxon panels that were installed in the rubble south of the CRI (Figure 29) also indicated these events on March 31 to April 4, and the other event beginning on April 28. Figure 31 shows the measured panel stress during the spring months. The two events were believed to be due to thermal and/or wind induced stresses (Frederking et al., 1988). During this time, Exxon panels 1 to 3 showed sporadic output (with pressures up to 2.5 MPa (Frederking and Sayed, 1988). Due to their sporadic nature, they are not included on Figure 31.

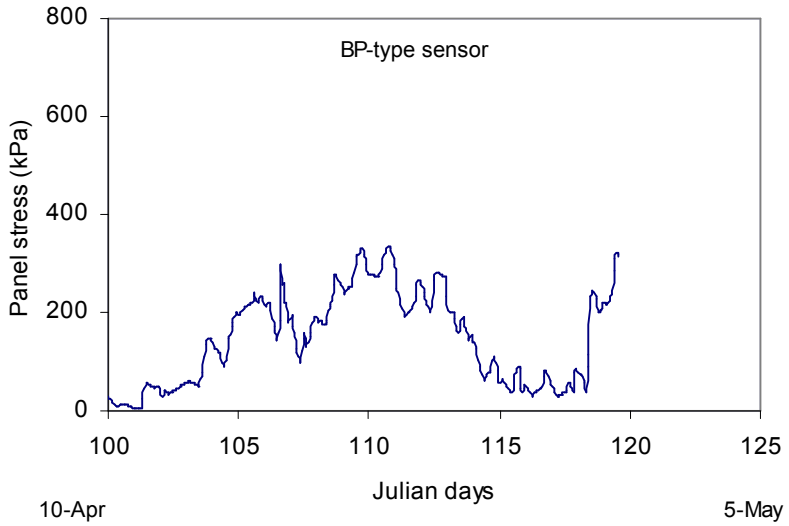

Figure 31: Output from the BP-type sensors installed south of the CRI at Kaubvik (after Marshal, 1990 with adaptations).

Examination of the load-time traces from the *in-situ* panels at Kaubvik (Figure 30) shows that there was little continuity between the same type of panel (in close proximity to one another) or different panels installed in the ice on the northwest quadrant of the CRI. There was no apparent trend of the lateral stress profile along radial lines throughout the rubble field. However, comparison of the individual panels suggests an attenuation of load due to the presence of grounded rubble (a trend similar to that experienced at Amerk).

5.4 Overview of Ice Loads on the CRI

Although there were a number of measurements of the local ice pressures, these measured local pressures were not converted to predict a global load on the CRI. Therefore no detailed measurements of global load are reported here.

6.0 MOLIKPAQ

6.1 Description of the Molikpaq

The Molikpaq structure was developed by Gulf Canada Resources Ltd. and operated by Beaudril, a subsidiary of Gulf. The Molikpaq is a Mobile Arctic Caisson (MAC) which was deployed in the Canadian Beaufort Sea in 1984 (Figure 32) and used for exploration drilling for four winter seasons in the Canadian Arctic (see Table 3). It consists of a continuous steel annulus on which sits a self-contained deck structure (Figure 33). The core of the annulus was filled with sand, which provided over 80 percent of the horizontal resistance. The outer face of the Molikpaq was designed for extreme ice features. The structure can operate without a berm in water depths ranging from 9 to 21 m. In water depths over this, the structure was designed to sit on a submerged berm that can vary in depth, as required. In deep waters, the angle of the outer face is 8°, whereas in shallower waters, the angle of the face is 23° (Figure 34). Ballasting of the caissons was entirely by water. To achieve the design resistance under dynamic load, densification of the hydraulically-placed core is required.

Figure 32: Photograph of the Molikpaq in the Canadian Beaufort Sea.

Table 3: Details of the Molikpaq deployment in the Beaufort Sea.

Site	Year Deployed	Water Depth (m)	Setdown Depth (m)	Subcut Depth Below Seabed (m)	Berm Height Above Seabed (m)	Core Height Above MSL (m)	Fill Quantity (m^3)
Tarsiut P-45	1984	25.5	19.5	3.5	6.0	2.0	450,000
Amauligak I-65	1985	31.0	19.5	9.0	11.5	1.5	1,400,000
Amauligak F-24	1987	32.0	15.8	16.0	16.2	4.8	2,200,000
Isserk I-15	1989	11.7	13.4	1.7	N/A	-3.8	70,000

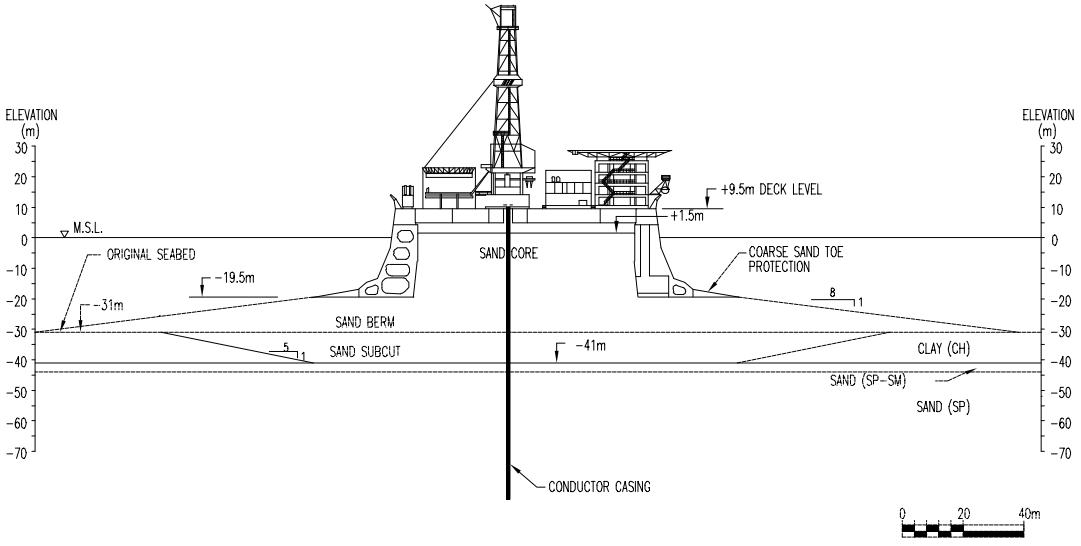

Figure 33: Cross-section view of the Molikpaq at the Amauligak I-65 site in 1985-86.

6.2 Instrumentation on the Molikpaq

An extensive array of sensors was installed on the structure to help assure operational safety as well as to provide collecting data for analysis purposes (Rogers et al., 1986, 1998). The Molikpaq was very well instrumented. A summary of the instrumentation is given in Table 4.

Table 4: Summary of Instrumentation on the Molikpaq.

Type of Instrument	Location	No.	Range	Resolution	Function
Medof Ice Panels	Caisson N, NE, E - Ice Faces	30	0-2000 Tonnes	1 Tonne	Ice Loads and Pressures
Strain Gauges	Caisson N, NE, E - Ice Face - Bulkheads - Sand Face - Base	60 168 24 30	±4140 ms	2 ms	Steel Strain and Stress
Extensometers	Caisson/Deck/Conductor Pipe	10	± 184 mm	1 mm	Caisson Deformations
Accelerometers	Caisson Core	18 2	±50% g	.025 % g	Tilt and Dynamic Response
Water Level Gauges	Ballast Tanks & Draft Levels	16	30 m	0.05 m	Water Levels
Total Pressure Cells	Caisson Base	40	± 3450 kPa	2 kPa	Base Contact Pressures
Piezometers	Caisson Sand Face Sand Core & Berm Foundations (Manual)	2 35 46	0-1035 KPa	1.7 kPa	Pore Water Pressures
Inclinometer	Core, Berm, Foundations (In-Place) Core, Berm, Foundations (Manual)	24 6	±2.5 Deg.	.002 Deg.	Lateral Deformation
Temperature Sensors	Medof Panels, Core, Berm	5 2	±100°C	.1°C	Temperature
Video Cameras	Derrick Top, NE Flare Boom	4	-	-	Film Documentation

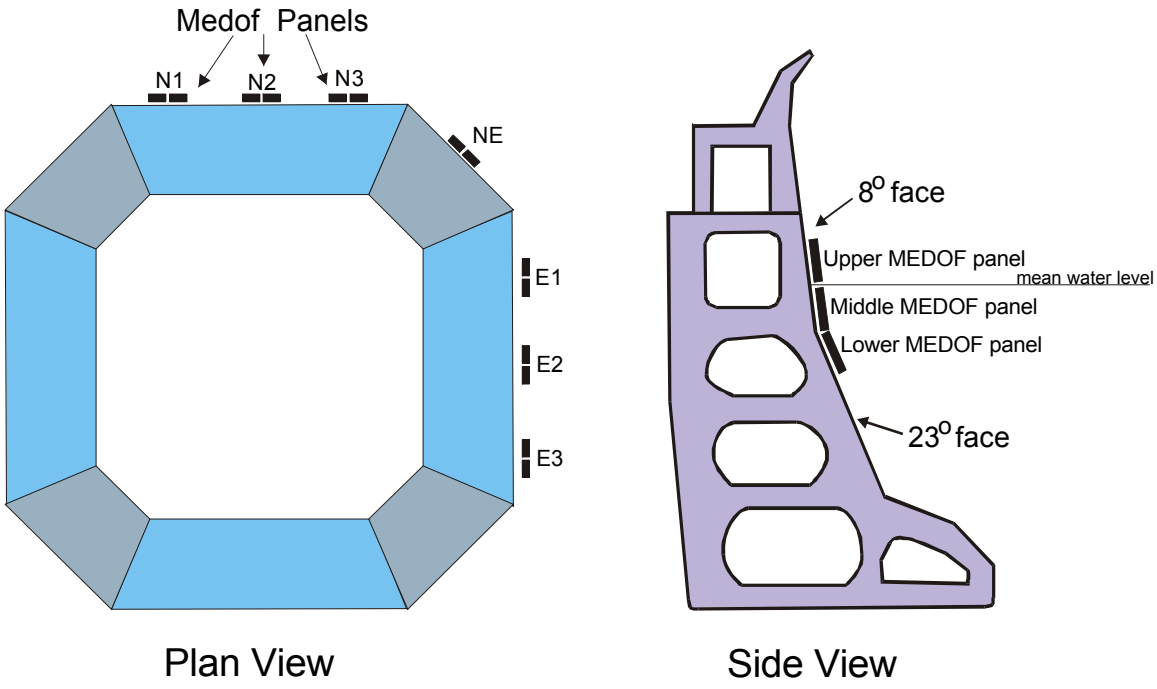

Figure 34: General location of the MEDOF panels on the Molikpaq. Each MEDOF panel sensor group has a sensing width of two panels, each 1.135 m wide and 2.7 m high. The detailed locations of individual panels are shown in Figure 35.

The MEDOF panels, strain gauges and extensometers have all been used to infer the ice loads. The loads predicted from all three types of instrumentation were quite comparable in a detailed analysis of the loading event. However, in most cases, the MEDOF panels gave more useful information since they also provided additional information on the loading character and location. Therefore the majority of the analyzed Molikpaq loading events were done using the MEDOF panels. In a few instances where high frequency loading occurred, the strain gauges provide more detailed information since they have a higher frequency response. Thus, a few events have used the strain gauge as the source of load measurement.

Thirty-one MEDOF panels were installed on the north, northeast and east faces of the caisson when the Molikpaq was built to provide a direct measure of ice load. The panels were arranged in 7 clusters of 4 or 5 panels. The locations of the MEDOF panels are shown in Figure 34 and Figure 35. Strain gauges were installed at the "09" location (Figure 36). Prior to April 12, 1986, there were 4 strain gauges, one along each side. After that date, an additional 12 gauges were installed. The locations of the 16 gauges are shown in Figure 36. Temperature sensors (RTD's) were embedded into the caisson outer plate directly behind several of the panels, which allowed thermal corrections to be made. Caisson loads were determined by integrating the measured ice loads across the face using the ice contact factors as observed on the video or by ice observers.

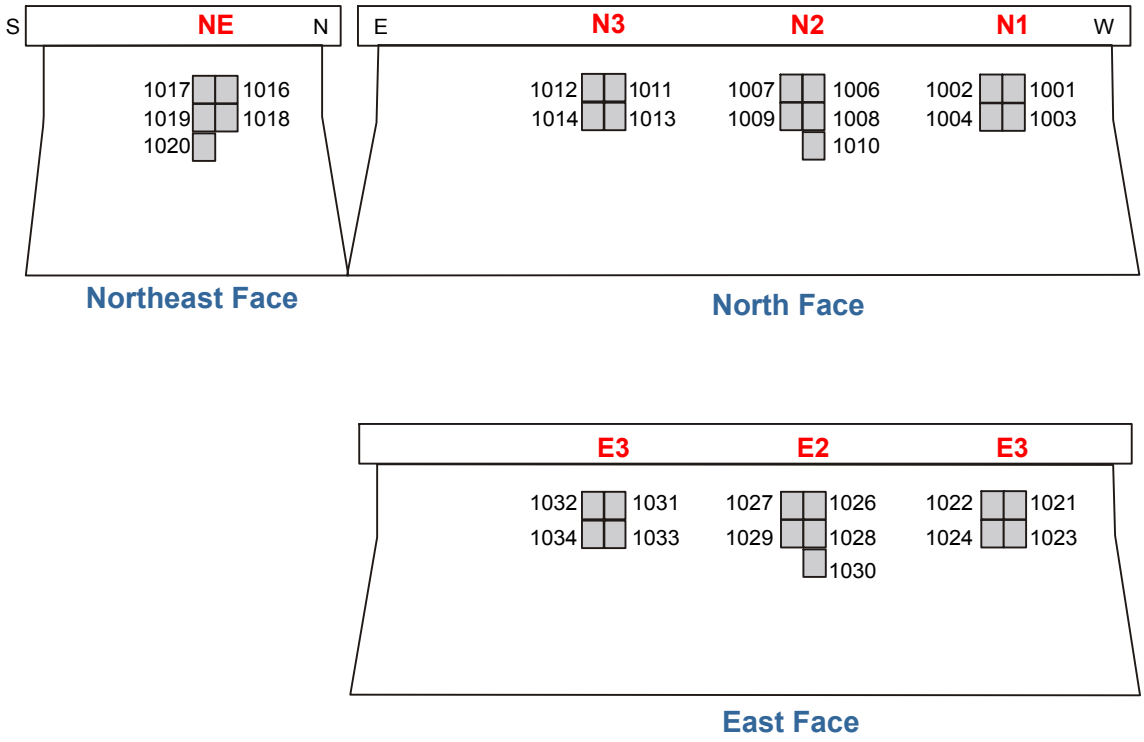

Figure 35: Location of the individual MEDOF panels on the Molikpaq.

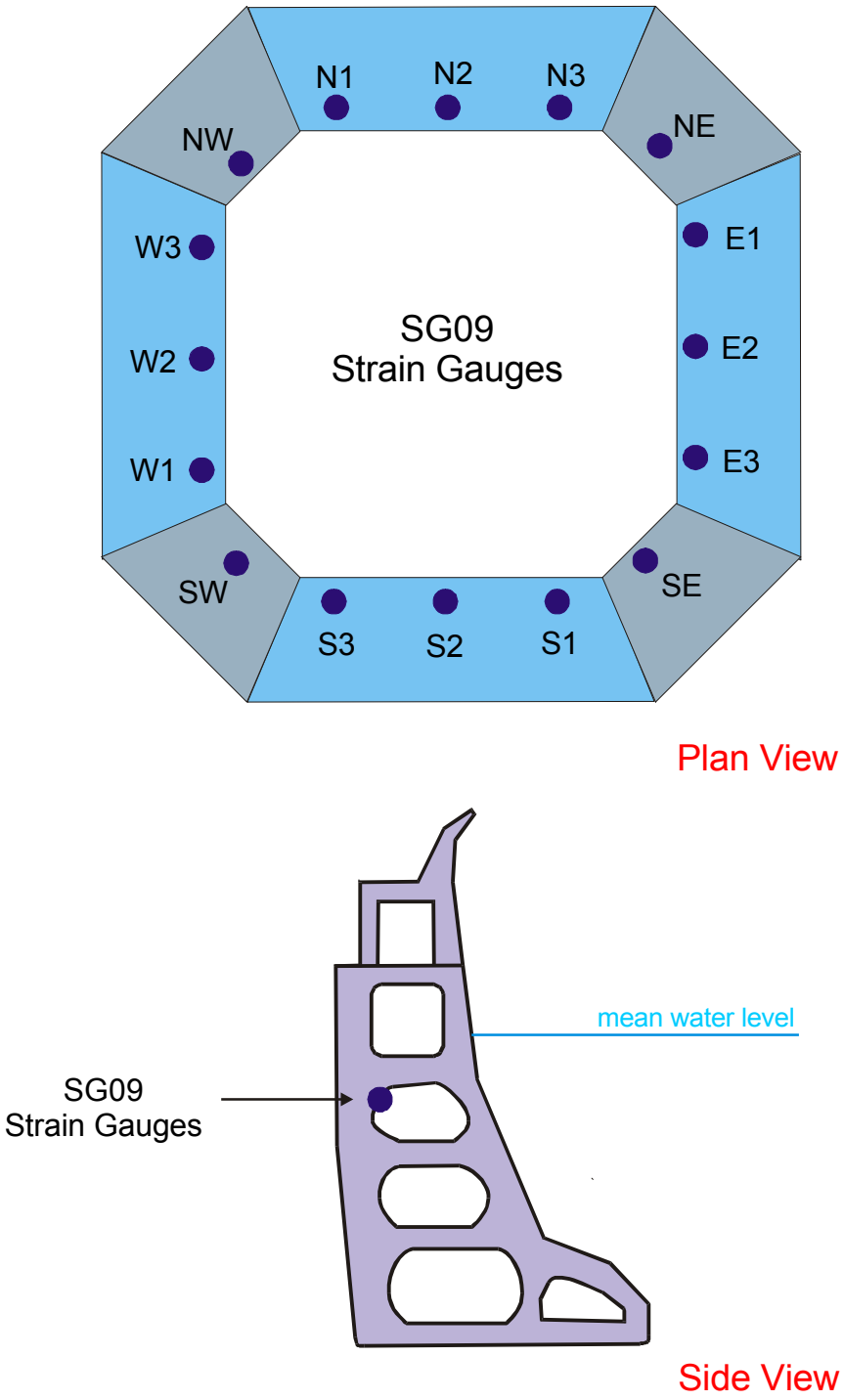

Figure 36: Locations of the 16 SG09 strain gauges on the Molikpaq.

Three modes of data acquisition were used on the Molikpaq to obtain the required information while remaining within the limit of the system. These modes were:

- **Slow** scanning (3 minute average, maximum and minimum on all channels) - Slow scanning was used for normal operations. Accelerometer and extensometer outputs were used to trigger a fast or burst scan rate if the threshold input was exceeded. Mode control was carried out by the HP 9920 computer and a rolling buffer scheme was used so that a few seconds of data leading to the trigger event was recorded as well as the post trigger period. This faster scan data was key to documenting the dynamic response of the Molikpaq.
- **Fast** scan rate (1 to 10 Hertz scanning of all channels) - The fast scan ran in parallel with the burst scanning. The fast scan provided higher frequency measurements of specific ice loading events. Its sampling rate provided relatively long scan duration, even though more transducer channels were being recorded. The limitation of the fast scan system was its inability to resolve the nature of the platform dynamics. It did, however, capture information related to the quasi-static loading.
- **Burst** scan rate (50 or 75 Hertz scanning of a key sub-set of channels) - The burst file used a sampling rate typically 50 times faster than the Fast scan so it was limited to a 90-second block. It gave a "snapshot" of a particularly dynamic response sequence. Furthermore, if the dynamic response became larger during the event, then a quasi-continuous record (to the limit of the storage media) was obtained.

The ice interaction with the Molikpaq was documented using a number of video cameras with real-time and time-lapse recorders. This information was extremely useful in documenting and describing different types of ice interaction and failure modes. Since the recorders put a “time-stamp” on the videos, individual loading events could be viewed on the videos. Detailed reports of ice information were also collected and this information was very valuable in analyzing the ice load events. The reports contained information on the ice drift speed and direction, ice thickness, rubble geometry, rubble block sizes, etc.

6.3 Calculation of Load

The MEDOF panels provided the most useful information on the ice loads. “Face” loads were determined from the measurement of loads on the individual MEDOF panels. To calculate the face loads, the loads in individual MEDOF clusters were first determined. There are three clusters of MEDOF Panels across each of the north and east faces (i.e. N1 - N2 - N3) with only one cluster on the northeast face (Figure 35). To determine the load on the north face, the load for each cluster area (i.e. N1, N2, N3) was derived from the panel loads in each cluster. Based on manual observations, a contact factor over the horizontal extent of each face segment is assigned uniquely for each ice event. This factor could range in value from 0 (i.e. no ice contact) to 1 (i.e. full contact). The results were summed to give the total measured face load. Since the panels did not cover the whole face, the summed load was factored up (increased) by the ratio of the face length (59 m) to the total panel width (7.11 m) on the face. The same procedure was used for the shorter northeast face by using appropriate length scale. Global loads were determined using the

vector sum of the individual face loads. Simple algebra was used to apportion the principal components of the loads on the short caisson faces. The loading direction was determined from the Arc Tangent of the two principal (N-S and E-W) load vectors.

6.4 Ice Conditions and Molikpaq Events

The Molikpaq was extensively instrumented and it was deployed in a wide variety of ice conditions. Consequently, the information from this structure is vitally important. It offers, by far, the best information on global loads on a wide offshore structure. In this section, the ice conditions and events for each of the four drill sites are detailed.

6.4.1 Tarsiut P-45

In 1984/85, during the first Molikpaq deployment at Tarsiut P-45 site, there were direct first year ice interactions with the near vertical caisson walls. Events at the Tarsiut P-45 site were characterized by ice ride-up, pile-up and crushing at the vertical caisson faces. Crushing was almost always observed when the leading edge of an impacting ice sheet contacted the caisson face (Neth, 1989). However, rubble pile formation was initiated by flexural failure of the host ice sheet. This produced both floating and grounded rubble piles. An important distinction between the two rubble formations was that the grounded rubble was able to sustain horizontal forces parallel to the caisson face due to surface traction between the grounded ice and the berm (Neth, 1989).

One of the major shortcomings of the data documentation for Tarsiut P-45 is the lack of detailed video coverage of the ice-structure and ice-rubble interactions (Neth, 1989). Video cameras were installed on the northeast flare boom on February 11, 1985. This provided valuable coverage of the north, northeast and east caisson faces. Video camera coverage from the derrick cameras was used for assessing the general ice conditions in the immediate vicinity of the rig.

Neth (1989) conducted an analysis of the Tarsiut P-45 data that emphasized rubble-building events. In all, 13 rubble-building events were identified after February 1985. Ice thickness for those events varied between 0.25 m and 1.2 m and ice drift speeds ranged from 0.05 to 0.25 m/s. A predominant southerly ice drift direction resulted in the formation of rubble piles along the north caisson wall in more than 50 % of the rubble events. Three of the 13 selected events, February 16, April 10 and April 11, were examined in detail by Neth (1989), due to their good visual ice documentation. A detailed examination of the ice failure modes from these three load records produced 18 individual ice loading events. Neth (1989) states that the ice forces associated with Tarsiut P-45 events were overestimated due to the availability of only slow 3-minute average data. Neth's analysis does not take into account the non-simultaneity of loading on the panels. It simply summed the peak values over 3-minute intervals. An analysis done by B. Wright (personal communication) showed that this type of analysis overpredicts the loads by a factor of two, and this has been taken into account for the loads for the Tarsiut P-45 location.

6.4.2 Amauligak I-65

In 1985-86, the Molikpaq was deployed at the Amauligak I-65 site. This site is close to the ice shear zone, and consequently the structure was subjected to a wide range of harsh ice conditions. This produced a unique data set on the various failure modes experienced during first and multi-year ice interaction with a vertically sided structure. Various failure modes were observed for the ice such as crushing, flexural, mixed modal, shearing, and creep. During the interaction with large ice features, there was often a large build-up of floating ice along the side of the Molikpaq.

The information from this site provided an extremely large number of ice loading events. To date, 167 events have been analyzed by the CHC from the Amauligak I-65 site. Considerably more data could be analyzed from this site. One hundred and fifty-seven of these events describe first-year ice features, and the other ten events were associated with multi-year ice features.

6.4.3 Amauligak F-24

In 1987-88, the Molikpaq was deployed in shallow water at the Amauligak F-24 site. At this site, the ice interacted with the 23° slope of the structure, rather than the 8° slope of the first two deployments (Figure 34). Early in the season, the ice was able to interact directly with the sloped caisson face, whereas later in the winter, the ice interacted with the grounded rubble field.

Ice loads at the Amauligak F-24 site were low which, considering the resolution of the instrumentation systems, limited the usefulness of that data. As a result, there are no quantified ice-loading Events from the Amauligak F-24 site.

6.4.4 Isserk I-15

In 1989-90, the Molikpaq was used to drill a well for Esso, Gulf and Chevron at the Isserk I-15 site, in a water depth of 11.5 m. Similar to the situation at the Amauligak F-24 site, the ice loading took place on the lower-sloped 23° face of the Molikpaq. During October and early November, the Molikpaq was exposed to mobile first year ice driven by strong winds. By November 10, however, the ice surrounding the Molikpaq had become quasi-stationary landfast ice. Subsequently, the loading was characterized by creep-type ice movement.

At this site, Esso Resources Canada Ltd. and partners collected data relevant to ice forces against an offshore structure surrounded by a grounded rubble pile. The structural instrumentation on the Molikpaq was supplemented at the Isserk site by *in-situ* load panels, a thermistor string and ice movement stations (Gulf Resources Canada 1990).

Only three ice-loading events were recorded for the Molikpaq at the Isserk site. These were all early winter events with relatively low load levels. The events resulted from the creep-type ice movement against the 23° sloped face. This induced flexural failures which, in conjunction with a partially grounded ice rubble, produced low loads (of the order of 10 to 35 MN).

6.5 Overview of Ice Loads on the Molikpaq

The ice load information for the Molikpaq was analyzed based on the type of ice feature loading the structure. The ice types that were identified were:

- Level, first-year sea ice
- Multi-year ice
- First-year ridges
- First-year hummock ice
- Isolated Floes (both first-year ice and multi-year ice)

Figure 37 shows a plot of the Line Load as a function of the ice thickness for the Molikpaq. The data in this plot are for loading events from level, first-year sea ice. The data has been subdivided into those cases where there was floating rubble surrounding the Molikpaq, and those cases in which the advancing ice sheet contacted the Molikpaq directly. In this case, Line-loads up to 2.5 MN/m were measured.

Figure 38 shows the Line Load as a function of the ice thickness for multiyear ice. In this case, very high Line-loads up to 8 MN/m were recorded. Note that in this case, the multi-year ice is significantly thicker than the first-year ice data shown in Figure 37.

Figure 39 shows the Line Load as a function of the sail height for first-year ridges. In this case, the Line Load ranged up to 1.1 MN/m for ridges with a sail height of 2 m.

Figure 40 shows the Line Load as a function of host ice thickness for hummocked ice. Line Loads ranged up to 2 MN/m. In all cases, there was no ice rubble surrounding the Molikpaq during these ice loading events.

Figure 41 shows the Line Load as a function of the average ice thickness for ice loading events in which a large isolated floe impacted the Molikpaq. The events with first-year ice show Line Loads up to 2 MN/m, whereas impacts from multi-year ice show Line Loads up to 3.5 MN/m.

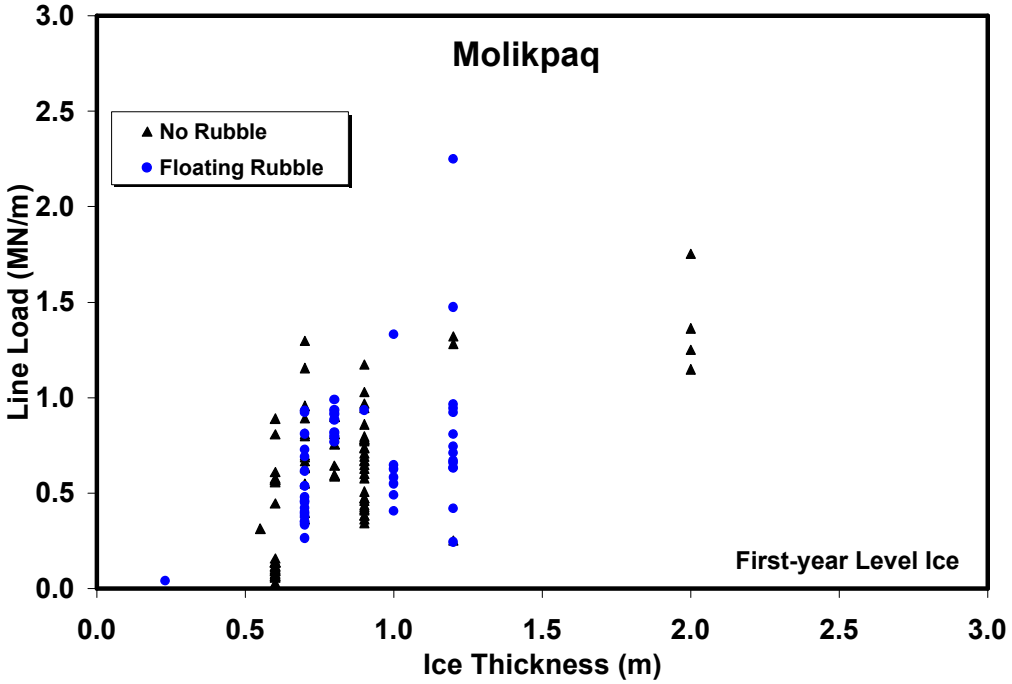

Figure 37: Line Load versus ice thickness on the Molikpaq. This plot shows only data relevant to level, first-year sea ice.

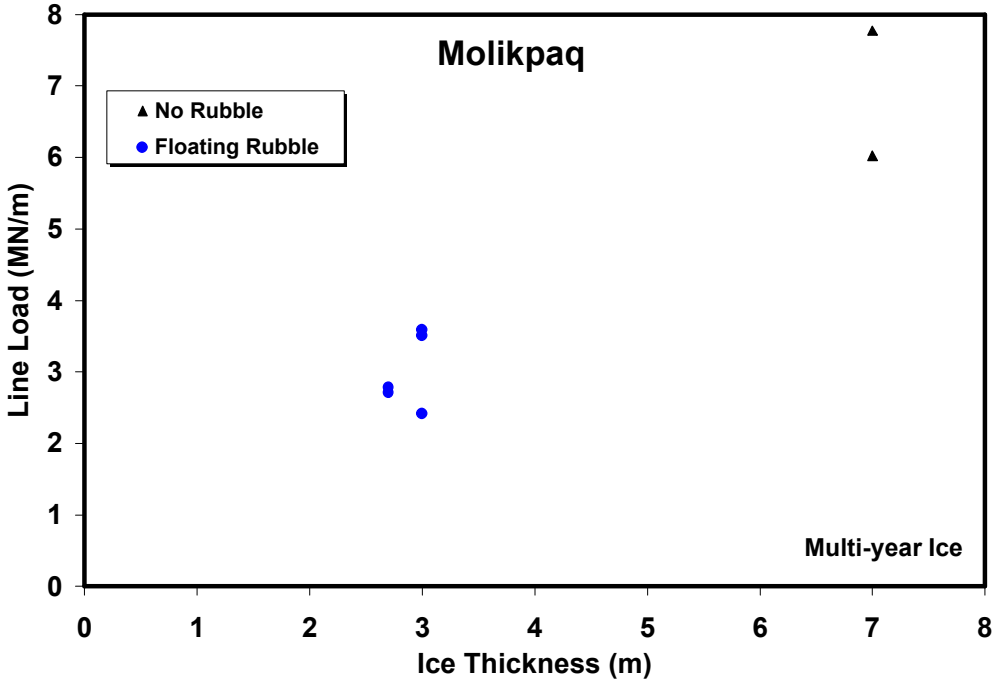

Figure 38: Line Load as a function of ice thickness for multi-year ice interacting with the Molikpaq

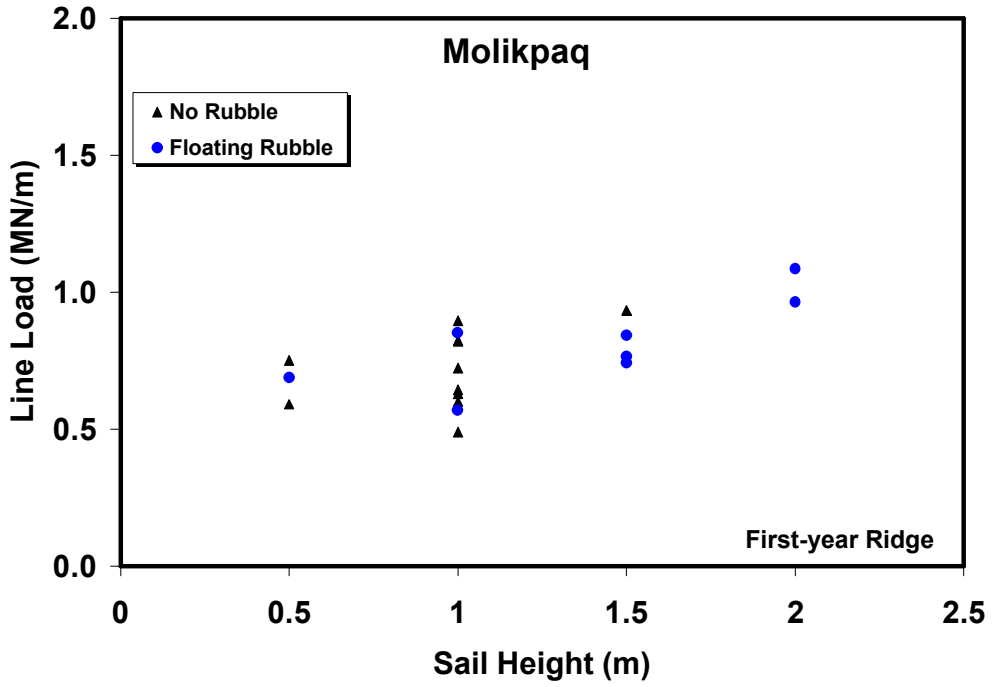

Figure 39: Line Load as a function of sail height for first-year ridge interaction with the Molikpaq.

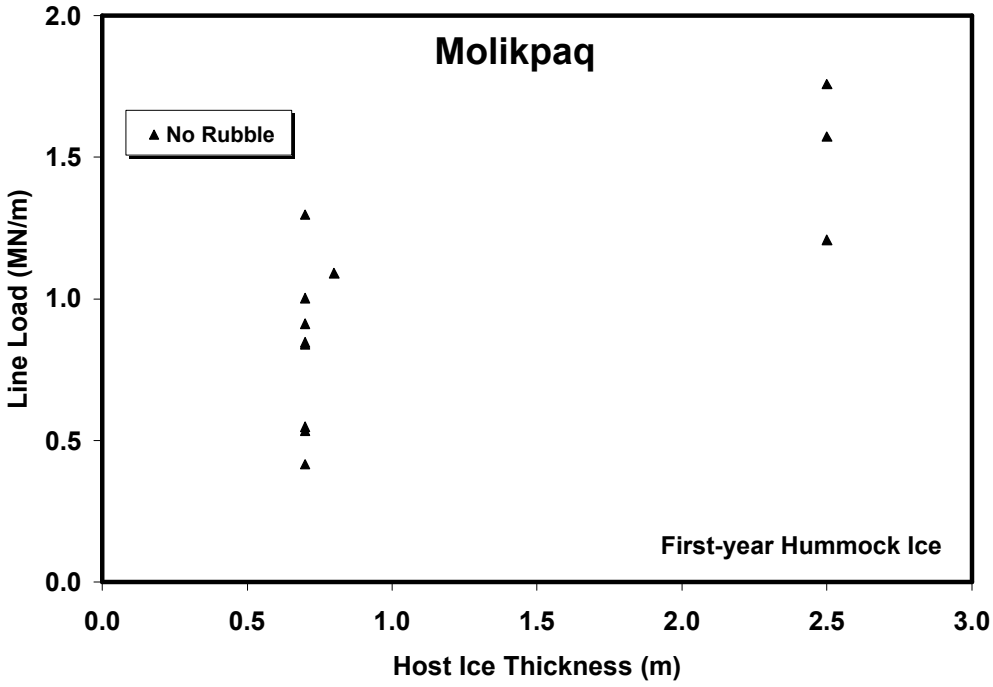

Figure 40: Line Load as a function of the host ice thickness for first-year hummock ice.

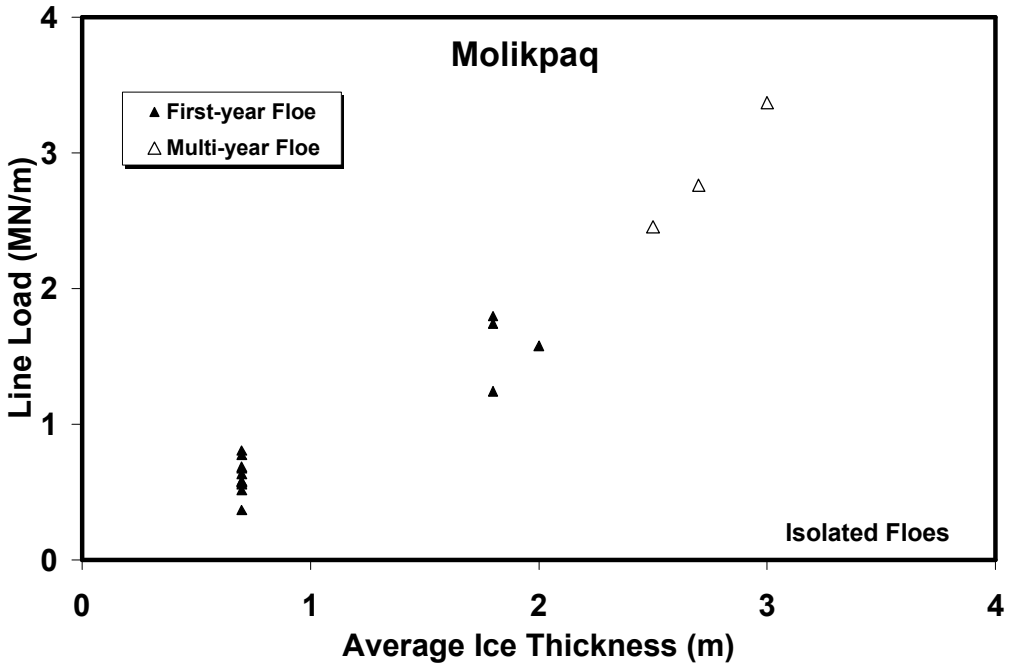

Figure 41: Line Load as a function of the average ice thickness of large isolated floes impacting the Molikpaq. The graph shows data for both first-year and multi-year ice.

7.0 GLOMAR BEAUFORT SEA 1 (CIDS)

This structure was operated by Global Marine in the American Beaufort Sea. It is made of a steel mud-base, concrete "brick" units through the ice zone and steel deck storage barges (see Figure 42). The steel units are not exposed to severe ice loading. The brick units are of a honeycomb construction that provide an optimum strength to weight ratio. The forces imposed by the ice are distributed evenly throughout the structure. The "silos" within the honeycomb structure are used only for water ballast, as are the tanks in the base. Ballast and deballast is entirely by water. The deballasting and reflotation process can be completed in three days under normal conditions. This structure was used only in the American Beaufort Sea.

Figure 42: Photograph of the CIDS in ice.

7.1 Overview of Ice Loads on the CIDS

Attempts to obtain detailed ice load information from this structure were not successful. There were anecdotal tales of a few significant ice loads events, but the details could not be found.

8.0 DISCUSSION

The information presented in the previous chapters has provided a great deal of information on the characteristics, use, and the ice loads on the caisson structures that were used in the Beaufort Sea. In this section, the data will be complied to present a more coherent view of the ice loads on these caisson structures.

8.1 Level First-year Sea Ice

8.1.1 Influence of Floating Rubble

Figure 43 and Figure 44 show the Line Load and Global Pressure, respectively, as a function of the ice thickness for all events with level ice loading the structures. The data have been subdivided according to whether or not there was floating rubble surrounding the structure. In the situation where there was no rubble, the level ice failed directly against the structure, whereas in those situations where a rubble field existed, the ice failure took place at the edge of the rubble. The data in the figures are further subdivided to show the events for both the Molikpaq and the SSDC.

From these figures there are several things to note.

- Although there is considerable scatter in the data, there does not appear to be a significant difference between the loads measured when floating rubble surrounded the structure and when it was absent. It is important to emphasize here that this rubble was floating and not grounded on the seabed. It appears that although grounded rubble has been shown to significantly attenuate the loads on a structure (Sayed, 1989), apparently floating rubble does not appreciably alter the load[5].
- There is a general increase in the Line Load with increasing ice thickness.
- There is no distinction between the data from the Molikpaq and the SSDC[6]. This is a very significant point. There has been considerable discussion, mostly outside the technical literature, that there was a large difference in the loads on these two structures. There has been considerable acrimony about this point. However, the present analysis has shown that there is little difference between the loads measured on these structures when viewed in terms of a Line Load and the appropriate ice thickness for loading.
- Although there is considerable scatter, there appears to be a general decrease in the Global Pressure with increasing thickness.
- The maximum Global Pressure that was measured was less than 2 MN/m^2. This point will be revisited later in this section.

[5]Note that this might not hold true if the rubble field is considerably wider than the structure, since, in that case, the rubble field could act as a "stress collector". There is some evidence of this at the Phoenix site of the SSDC.

[6] The data points for the SSDC with low load levels represent the loading situations with a very large rubble field surrounding the structure. Although the rubble was mostly floating, there were grounded portions and this would reduce the load on the structure.

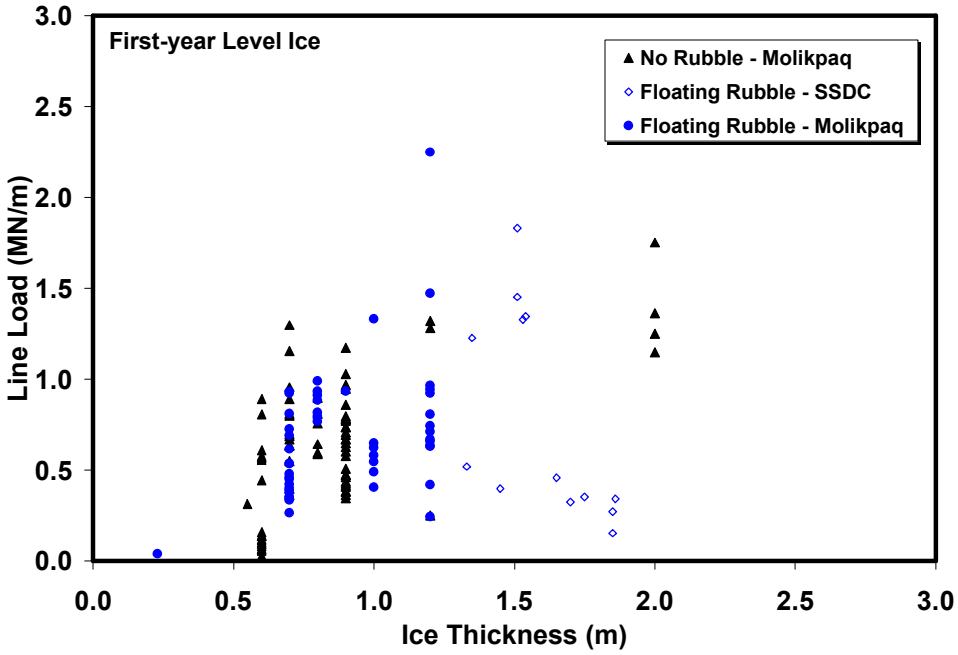

Figure 43: Line Load as a function of ice thickness for first-year level ice. The figure shows that there is little influence of floating rubble on the loads on the structure.

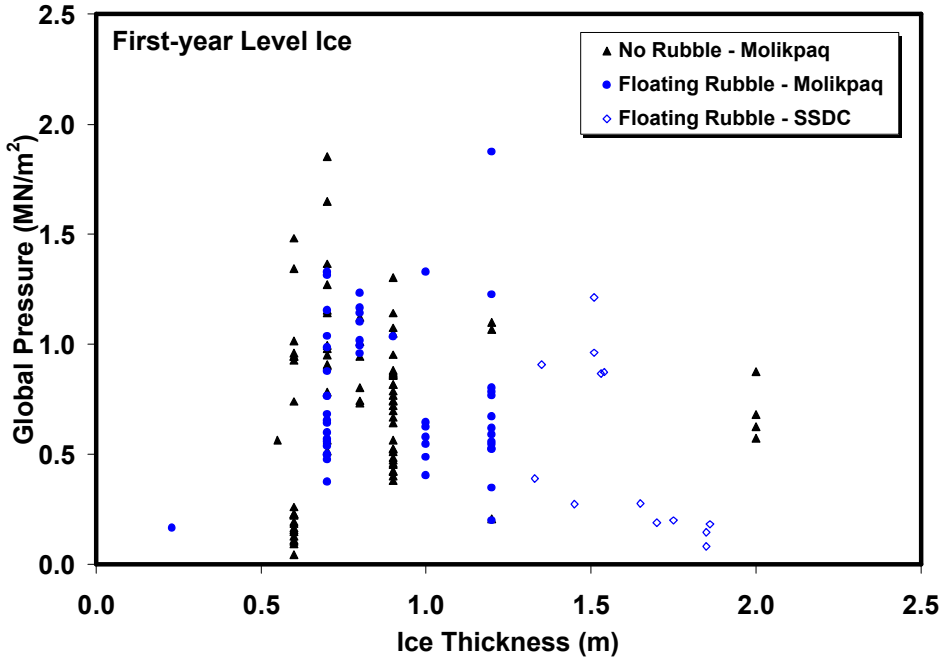

Figure 44: Global Pressure versus ice thickness for level first-year sea ice.

8.1.2 Failure Modes

Various failure modes were observed for the ice during the interaction process with the structure. These failure modes included crushing (Figure 45), flexural (Figure 46), mixed modal (Figure 47) and creep. During the interaction with large ice features, there was often a large build-up of ice along the side of the Molikpaq (Figure 48).

It is instructive to view the ice loading events in terms of the failure mode of the ice. Figure 49 shows the Line Load as a function of the ice thickness where the data points have been subdivided to show the failure mode of the ice during the interaction event. This figure clearly shows that the failure mode directly influences the load on the structure. For a constant ice thickness, the loads increase as the failure mode changes from flexure, to mixed-mode, to crushing. This explains the wide scatter observed in the data (Figure 43 and Figure 44).

Figure 50 and Figure 51 show the Global Pressure as a function of the time-to-failure and the average loading rate during the interaction event, respectively. The data in the figures are subdivided according to their failure mode. These figures again clearly show the influence of the failure mode on the load on the structure. Figure 51 shows that there is a general trend of increasing load with increasing loading rates.

Figure 45: Crushing along the corner of the Molikpaq. Note that the large build-up of ice rubble has caused a subsequent large flexural failure of the ice sheet.

Figure 46: Local flexural failures along the side of the Molikpaq.

Figure 47: Mixed mode failure along the side of the Molikpaq. Note the large cracks in the parent ice sheet.

Figure 48: Pile-up alongside the Molikpaq.

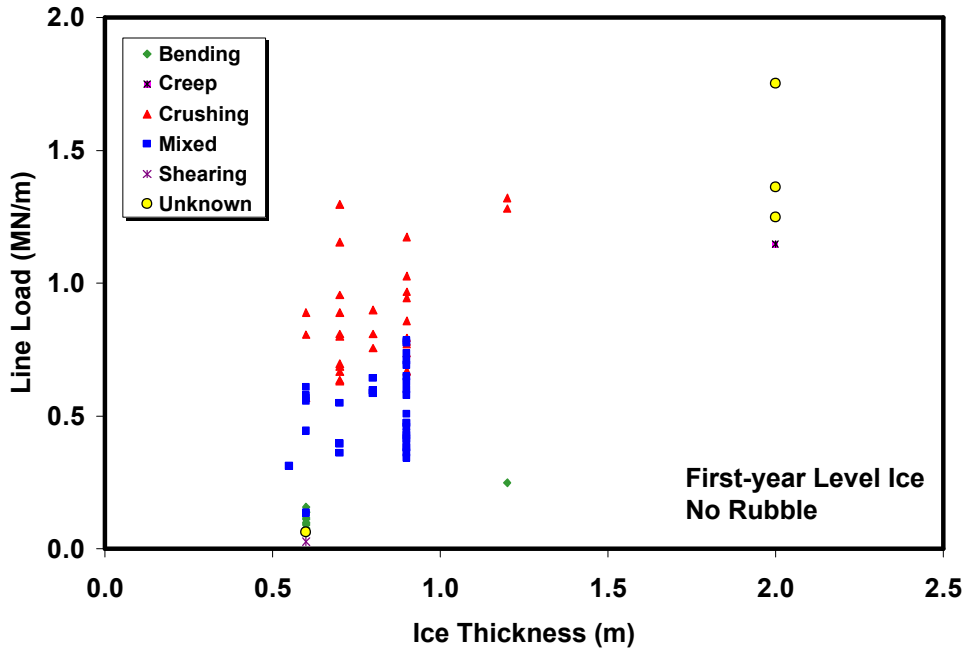

Figure 49: Line Load as a function of ice thickness showing the influence of the failure mode of the ice on the measured load.

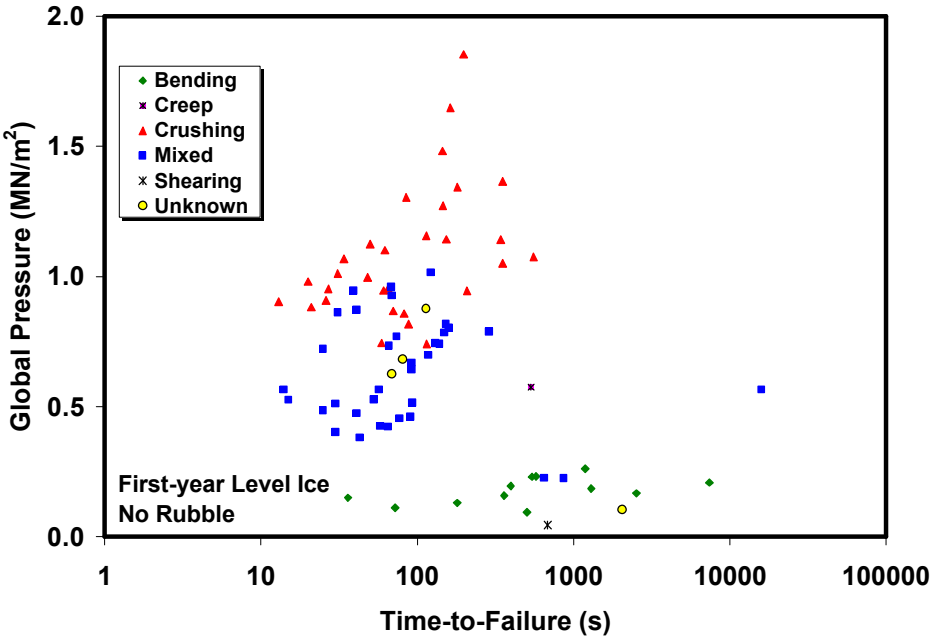

Figure 50: Global Pressure versus the time-to-failure for first-year sea ice.

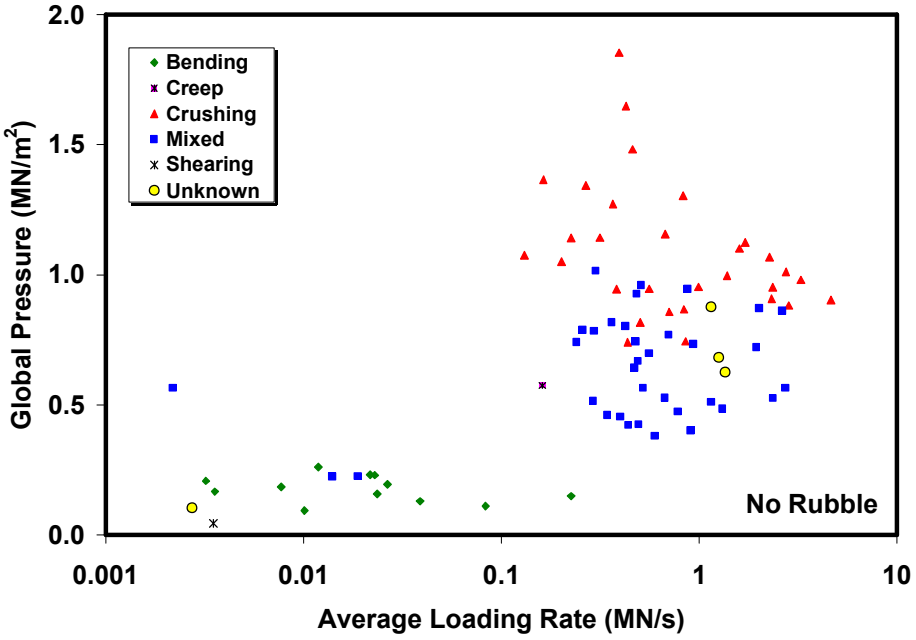

Figure 51: Global Pressure versus the average loading rate for first-year level sea ice.

Figure 52 shows the Line Load and associated failure modes observed during the interaction of first-year hummock ice. All of these events were recorded on the Molikpaq. In this case, the loads due to creep failure were the highest loads recorded. However, this occurred with significantly thicker ice than those events where other failure modes were observed. Similar to the level ice, the crushing failure gave the highest loads for a given ice thickness where different failure modes were observed.

Figure 53 shows the Line Load and the associated failure modes observed during the impact of isolated floes of first-year ice impacting the Molikpaq. For many of these cases, the failure mode of the ice was not known.

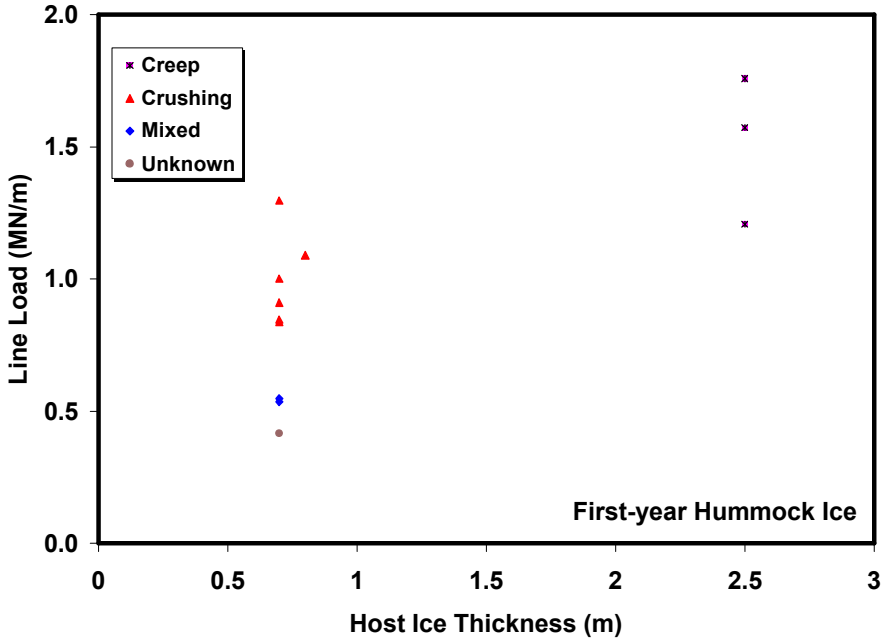

Figure 52: Line Load as a function of the host ice thickness for first-year hummock ice showing the associated failure modes for the ice.

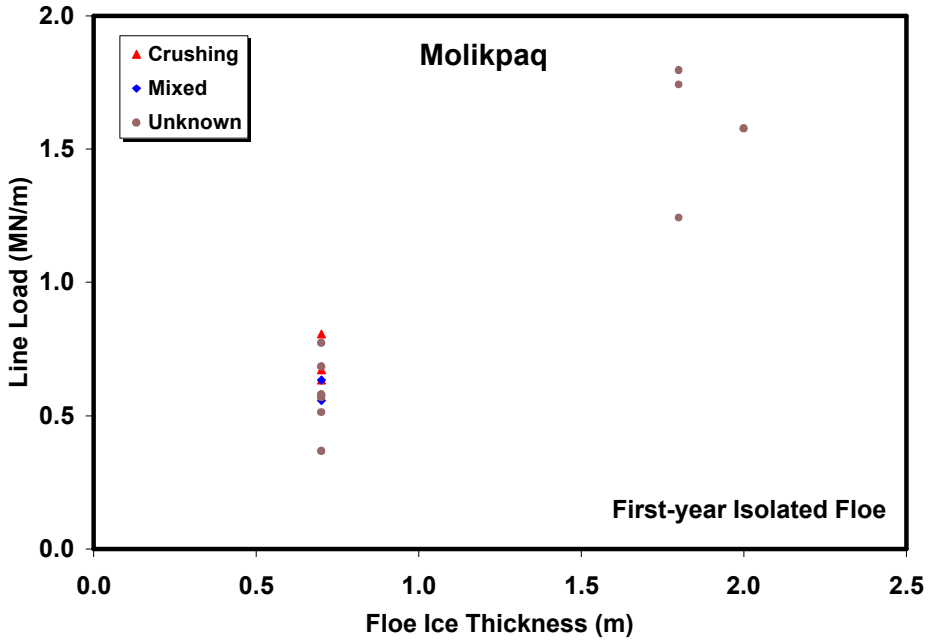

Figure 53: Line Load as a function of the floe ice thickness for first-year isolated floes showing the associated failure modes for the ice.

8.2 Ice Macrostructure

The offshore structures in the Canadian Beaufort Sea were subjected to a wide variety of ice conditions including level first-year sea ice, first-year hummock and ridge ice, isolated ice floes, and multi-year sheet ice. Throughout this report, the data from these ice macrostructures have been presented individually. In this section, a comparison will be made of the loads generated by these ice macrostructures.

Figure 54 shows a plot of the Line Load as a function of ice thickness for all ice macrostructures (except ridges) for first-year ice only. Although there is scatter, it is evident that all of the data are quite comparable. The data for all three structures are in good agreement, especially if consideration is given to the influence of the grounded rubble surrounding the Tarsiut and SSDC. There is a general increase in the Line Load with increasing ice thickness. It should be noted that although the data for the ridges could not be presented on this plot (since it cannot be related to an ice thickness). Previous analysis of ridge loads by Wright and Timco (2000) has shown that the ridge loads are less than those generated by ice crushing events of level ice.

Figure 55 shows a plot of the Line Load as a function of ice thickness for all ice macrostructures (except first-year ridges) for both first-year and multi-year ice. The trend shown in Figure 54 of increasing Line Load with increasing ice thickness is continued with the thicker multi-year ice.

Figure 56 shows a plot of the Global Pressure as a function of ice thickness for all ice macrostructures (except ridges) for first-year ice only. There is considerable scatter in the data, but no significant differences amongst the global pressures measured on the three caisson structures. It is significant to note that no Global Pressures above 2 MN/m^2 were measured on any structure with loading from first-year sea ice.

Figure 57 shows a plot of the Global Pressure as a function of ice thickness for all ice macrostructure (except first-year ridges) for both first-year and multi-year ice. The data for the multi-year ice appear to be higher than for first-year ice for the same ice thickness. However, there is quite good general agreement amongst all of the data. The figure shows a very significant feature – there are no recorded events in which the Global Pressure on the structure exceeded 2 MN/m^2.

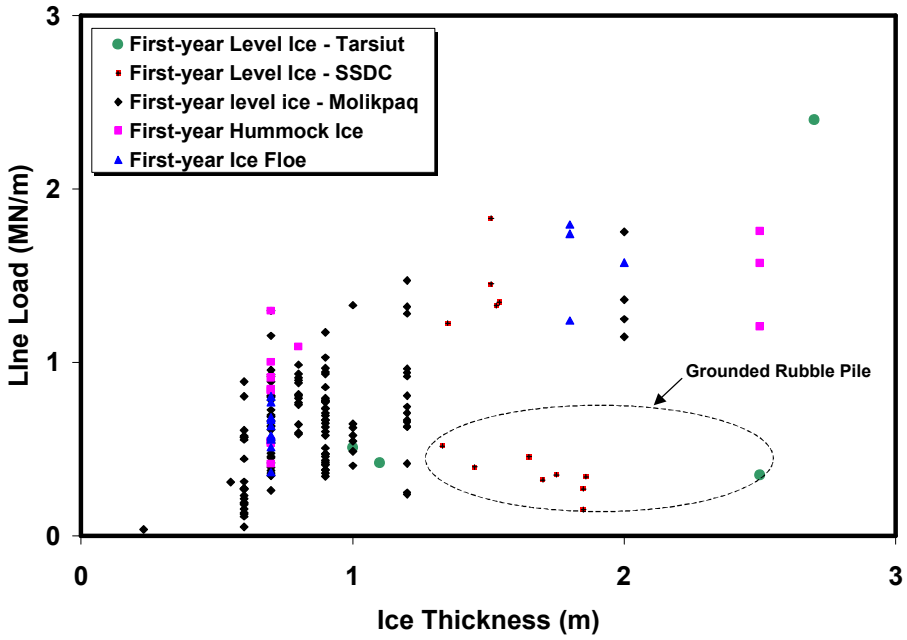

Figure 54: Line Load as a function of ice thickness for different ice macrostructures for first-year ice only.

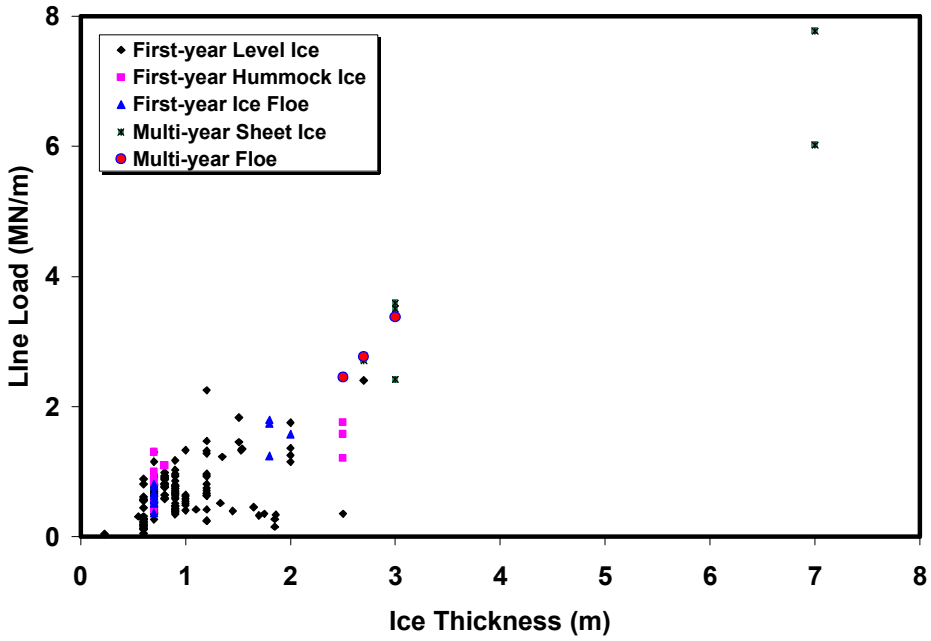

Figure 55: Line Load as a function of ice thickness for different ice macrostructure for both first-year and multi-year ice.

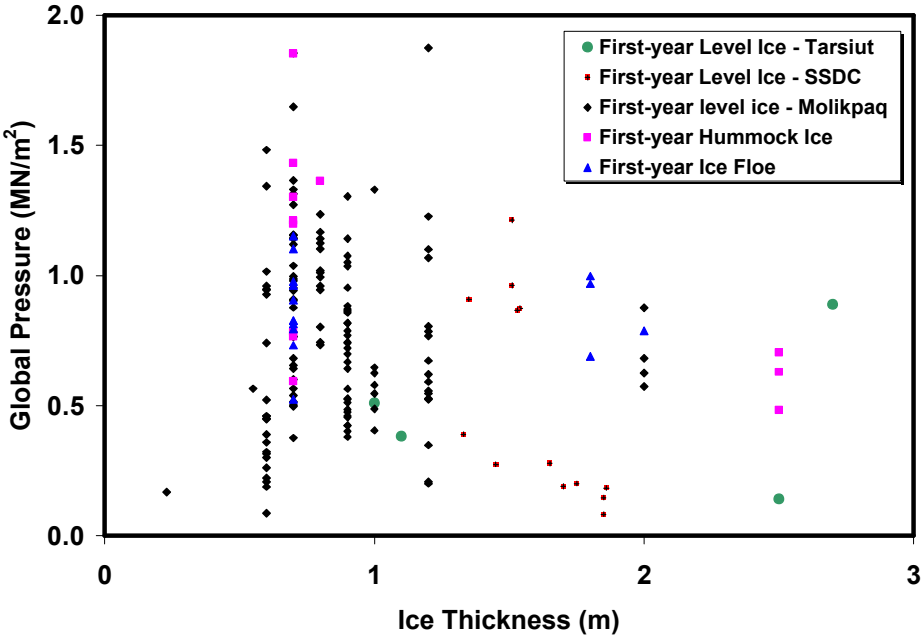

Figure 56: Global Pressure as a function of ice thickness for different ice macrostructure for first-year ice only.

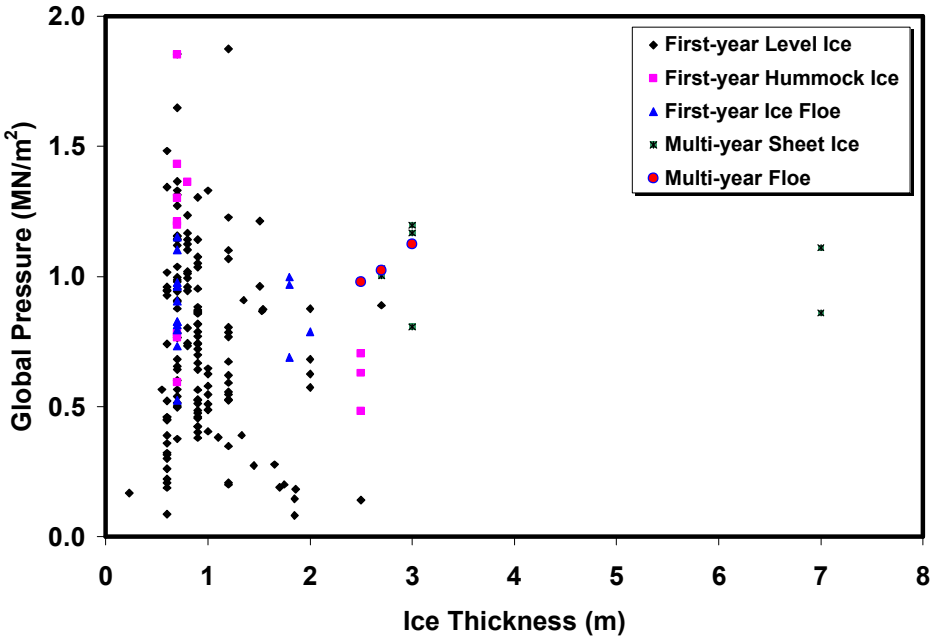

Figure 57: Global Pressure as a function of ice thickness for different ice macrostructures for both first-year and multi-year ice.

9.0 SUMMARY

This report has presented an overview of the five caisson structures that were used in the exploration drilling of the Beaufort Sea in the 1980s. Details are presented on the characteristics, instrumentation and measured ice loads on the Tarsiut Caissons, the Single Steel Drilling Caisson (SSDC), the Caisson Retained Island (CRI), and the Molikpaq. General information, but no ice loads, has been presented on the Glomar Beaufort Sea 1 (CIDS). The global loads on the structures have been presented as a Line Load (Global Load per width of the structure) and the Global Pressure (Line Load per ice thickness). The analysis has shown:

- A large amount of information on global loads has been obtained form the Molikpaq. Considerably less information is available from the SSDC and Tarsiut caisson. There is no global load event information for the CRI or CIDS.
- Analysis of the global load in terms of a Line Load or Global Pressure provides a convenient method to compare and correlate data.
- There is a general increase in the Line Load with increasing ice thickness.
- The Line Load was less than 1 MN/m in the majority of loading events.
- Floating rubble does not appear to appreciably alter the loads on the structure (compared to cases where no rubble exists). However, the presence of rubble can influence the failure mode of the ice and keep the ice loading "at a distance" from the structure face.
- There is no significant difference in the data measured on any of the structures, if the ice thickness and failure mode are considered in the analysis.
- Global loads are a function of the ice macrostructure (level first-year sea ice, multi-year ice, first-year ridges, hummock fields, isolated floes).
- Although the data show considerable scatter, much of the scatter can be explained by examining the failure mode of the ice during the interaction process.
- A significant result of the analysis is that the Global Pressure measured for all types of ice loading events on caisson structures never exceeded 2 MN/m^2.

10.0 REFERENCES

Blanchet, D. and Keinonen, A. 1988. Ice Load Measurements at Phoenix, Harrison Bay Winter 1986-87. Canmar/Valmet Report, 208 pp., Calgary, Al., Canada.

Blanchet, D. and Wiefelspuett, R. 1988. Ice Load Measurements at Aurora, Beaufort Sea Winter 1987-88. Canmar/Wartsila Report, 95 pp., Calgary, Al., Canada.

Canmar 1985. Kogyuk Stability Monitoring Program 1983-84: Event Data, Vol. I4 - I6. Calgary, Al., Canada.

Cox, G. 1984. Evaluation of a Biaxial Ice Stress Sensor. Proceedings of 7th International Symposium on Ice (IAHR), Vol. II, pp. 340-361, Hamburg, Germany.

Cox, G. 1987. Kadluk Ice Stress Measurement Program. *in* Technology Assessment and Research Program for Offshore Minerals Operation, J. Gregory, Ed., MMS Report 42-1494, pp 100-107, Washington, DC, USA.

Croasdale, K. 1985. Ice Investigations at a Beaufort Sea Caisson. K.R. Croasdale and Associates, Ltd. (KRCA) Report to Public Works Canada, Calgary, Al., Canada.

Croasdale, K., Der, C.D. and Shinde, S.B. 1988. Ice Forces and Geotechnical Response of the Esso Caisson Retained Island, 1986-87. Esso Resources Canada Ltd. Report, Calgary, Al., Canada.

Croasdale, K.R.. and Frederking, R.M.W. 1986. Field Techniques for Ice Force Measurements. Proceedings IAHR Ice Symposium, Vol. 2, p. 443-482, Iowa City, Iowa, USA.

Frederking, R.M.W and Sayed, M. 1988. Measurements of Ice Load Transmission through Grounded Rubble, Kaubvik I-43, 1987. National Research Council of Canada Report to Canadian Oil and Gas Lands Administration - Energy, Mines and Resources Canada, Ottawa, Ont., Canada.

Frederking, R.M.W., Sayed, M., Wessels, E., Child, A.J. and Bradford, D. 1984. Ice Interaction with Adams Island, Winter 1982-83. Proceeding of 7th International Symposium on Ice (IAHR), Vol. III, pp. 187 – 201, Hamburg, Germany.

Frederking, R., Timco, G.W. and Wright, B.D. 1999. Ice Pressure Distribution from First-Year Sea Ice Features Interacting with the Molikpaq in the Beaufort Sea. Proceedings 9th International Offshore and Polar Engineering Conference ISOPE'99, Vol II, pp 541-548, Brest, France.

Graham, B., Chabot, L. and Pilkington, R. 1983. Ice Load Sensors for Offshore Arctic Structures. Proceedings of 7th International Conference on Port and Ocean Engineering under Arctic Conditions Vol. IV, pp. 547 - 562, Espoo, Finland.

Gulf Resources Canada, 1990. Molikpaq at Isserk I-15, 1989-90: Operations Report, Volume 1, Calgary, Al., Canada.

Hawkins, J.R., James, D.A. and Der, C. 1983. Design, Construction and Installation of a System to Measure Environmental Forces on a Caisson Retained Island. Proceedings of 7th International Conference on Port and Ocean Engineering under Arctic Conditions Vol. IV, pp. 770 - 779, Espoo, Finland.

Hewitt, K., Berzins, W., Fitzpatrick, J. and Hogeboom, G. 1985. The Design, Installation and Performance of a Berm Supported Exploration Structure in the Beaufort Sea. Proceedings 4th Offshore Mechanics and Arctic Engineering Symposium, Vol. II, pp. 105-113, Dallas, Texas, USA.

Hewitt, K.J., Sladen, J.A., Williams, D.R. and Brown, J. 1988. Geotechnical Evaluation and Performance of the Canmar SSDC/MAT Mobile Offshore Drilling Unit. Proceedings 41st Geotechnical Conference, pp. 364-372, Kitchener, Ont., Canada.

Jahns, H.O. 1985. Offshore Outlook - Technological Trends American Arctic. OMAE Panel Session, Dallas, TX, USA.

Johnson, J.B., Cox, G.F.N. and Tucker, W.B. 1985. Kadluk Ice Stress Measurement Program. Proceedings of 8th International Conference on Port and Ocean Engineering (POAC), Vol. I, pp. 88-100, Greenland.

Mancini, C.V., Dowse, B.E. and Chevallier, J.M. 1978. Caission Retained Island for Canadian Beaufort Sea - Geotechnical Design and Construction Considerations. Proceedings of Offshore Technology Conference, Paper no. 4581, pp. 17 – 22, Houston, Texas, USA.

Marshall, A. 1990. A Theoretical and Field Study of Load Transmission through Grounded Ice Rubble. M.Eng.thesis, 169 pp, Memorial University of Newfoundland, St. John's, Nfld., Canada.

Masterson. D. et al. 1991. Beaufort Sea Exploration: Past and Future. Offshore Technology Conference paper OTC6530, Houston, Texas, USA.

Neth, V. 1989. Rubble Formation along the Molikpaq at Tarsiut P-45 during 1984-85. Gulf Canada Resources Ltd. Report to the NRC, Calgary, Al, Canada.

Pilkington, G.R. et al. 1986. A Review of the Kulluk's Performance after Three Years Operating in the Beaufort Sea. Proceedings IAHR Symposium on Ice, Vol. 3, pp 145-176, Iowa City, Iowa, USA.

Pilkington, G.R., Blanchet, D., and Metge, M. 1983. Full Scale Measurements of Ice Forces on an Artificial Island. Proceedings of 7th International Conference on Port and Ocean Engineering under Arctic Conditions Vol. IV, pp. 818-834, Espoo, Finland.

Poplin, J.P. 1990. Nipterk P-32 Spray Ice Island. Esso Report ERCL.RS.89.24, Calgary, Alberta, Canada.

Ralston, T.D. 1979. Sea Ice Loads. *in* Technical Seminar on Alaskan Beaufort Sea Gravel Island Design. Exxon Company, Houston, Texas, USA.

Sayed, M. 1989. Transmission of Loads through Grounded Ice Rubble. *in* 4th IAHR State-of-the-Art Report on Ice Forces on Structures, *G.W. Timco, Ed.*, USA CRREL Special Report 89-5, pp 259-275, Hanover, NH, USA.

Sayed, M., Frederking, R.M.W. and Croasdale, K.R. 1986. Ice Stress Measurements in a Rubble Field Surrounding a Caisson-Retained Island. Proceeding of 1st International Conference on Ice Technology, pp. 255-262, Boston, Mass., USA.

Timco, G.W. 1998. NRC Centre for Ice Loads on Offshore Structures. NRC Report HYD-TR-034, Ottawa, Ont., Canada.

Timco, G.W. 1996. NRC Centre of Ice/Structure Interaction: Archiving Beaufort Sea Data. Proceedings 13th IAHR Symposium on Ice, Vol. 1, pp 142-149, Beijing, China.

Timco, G.W. and Wright, B.D. 1999. Load Attenuation through Grounded Ice Rubble at Tarsiut Island. Proceedings 15th International Conference on Port and Ocean Engineering under Arctic Conditions, POAC'99, Vol. 1, pp 454-463, Helsinki, Finland.

Timco, G.W., Johnston, M. and Frederking, R. 1999a. The NRC Ice Load Catalogue. Proceedings 15th International Conference on Port and Ocean Engineering under Arctic Conditions, POAC'99, Vol. 1, pp 444-453, Helsinki, Finland.

Timco, G.W., Wright, B., Johnston, M. and Frederking, R. 1999b. First-Year Ice Ridge Loads on the Molikpaq. Proceedings 4th International Conference on Development of the Russian Arctic Offshore, RAO99, Part II, pp 172-179, St. Petersburg, Russia.

Wright, B.D., 2001. Ice Loads on the Kulluk in Managed Ice Conditions. Proceedings POAC'01, Vol. 2, pp 553-565, Ottawa, Canada

Wright, B.D., 2000. Full Scale Experience with Kulluk: Stationkeeping Operations in Pack Ice. B. Wright & Associates, Canmor, Al., PERD/CHC Report 25-44.

Wright, B.D. and Timco, G.W. 2000. First-year Ridge Interaction with the Molikpaq in the Beaufort Sea. Cold Regions Science and Technology 32, pp 27-44.

REPORT DOCUMENTATION FORM/FORMULAIRE DE DOCUMENTATION DE RAPPORT

REPORT No./ N°. DU RAPPORT	PROJECT No./ N°. DU PROJET	SECURITY CLASSIFICATION/ CLASSIFICATION DE SÉCURITÉ
CHC-TR-003	Project 63000/61800	__ Top Secret/Très sécret __ Secret __ Confidential/Confidentiel __ Protected/Protégée _x_ Unclassified/Non classifiée
DISTRIBUTION/DIFFUSION __ Controlled/Contrôlée _x_ Unlimited/Illimitée		

DECLASSIFICATION: DATE OR REASON/DÉCLASSEMENT: DATE OU RAISON

TITLE, SUBTITLE/TITRE, SOUS-TITRE

Caisson Structures in the Beaufort Sea 1982-1990:
Characteristics, Instrumentation and Ice Loads

AUTHOR(S)/AUTEUR(S)

G.W. Timco and M.E. Johnston

SERIES/SÉRIE

Technical Report

CORPORATE AUTHOR/PERFORMING ORGANIZATION/
AUTEUR D'ENTREPRISE/AGENCE D'EXÉCUTION

Canadian Hydraulics Centre
National Research Council of Canada

SPONSORING OR PARTICIPATING AGENCY/AGENCE DE SUBVENTION OU PARTICIPATION

Program of Energy Research and Development (PERD)

DATE	FILE/DOSSIER	SPECIAL CODE/ CODE SPÉCIALE	PAGES	FIGURES	REFERENCES
Nov, 2002			72	57	

NOTES

DESCRIPTORS (KEY WORDS)/MOTS-CLÉS

Ice loads, Beaufort Sea, caisson structures

SUMMARY/SOMMAIRE
This report presents an overview of ice loads on Beaufort Sea caisson structures.

ADDRESS/ADDRESSE
Canadian Hydraulics Centre
National Research Council of Canada
Montreal Road, Ottawa, K1A 0R6, Canada
(613) 993-2417